Textural Sector-Zoning in Garnet: Theoretical Patterns and Natural Examples from Alpine Metamorphic Rocks

A. Hugh N. RICE[1)*)], Gerlinde HABLER[2)], Elisabeth CARRUPT[3)], Gianluca COTZA[1)], Gerhard WIESMAYR[4)],
Ralf SCHUSTER[5)], Helmut SÖLVA[6)], Martin THÖNI[2)] & Friedrich KOLLER[2)]

[1)] Department of Geodynamics and Sedimentology, Geozentrum, Althanstraße 14, 1090 Vienna, Austria.

[2)] Department of Lithospheric Research, Geozentrum, Althanstraße 14, 1090 Vienna, Austria.

[3)] Department of Geology, University of Lausanne, Lausanne, Switzerland.

[4)] Rohöl-Aufsuchungs AG, Schwarzenbergerplatz 16, A-1015 Vienna, Austria.

[5)] Geologisches Bundesanstalt, Neulinggasse 38, 1031 Vienna, Austria.

[6)] Institute of Earth Sciences, University of Graz, Heinrichstraße 26, 8010 Graz, Austria.

[*)] Corresponding author, alexander.hugh.rice@univie.ac.at

Abstract

In pelitic rocks, textural sector-zoning occurs together with displacement of insoluble matrix grains, especially graphite; this requires a lithostatic (non-differential) stress with a high fluid-pressure, making it an indicator of non-kinematic growth. Theoretical sector-zoning patterns in garnet depend on the section orientation and the crystal form; combined rhombdodecahedral-icositetrahedral forms can have at least 20 sectors. In thin-sections, the width of type-1 (matrix-derived) inclusions along sector boundaries depends on the angle the section makes through the boundary. The observed length of type-2 intergrowths lying (sub-) normal to crystal faces forming the base of that growth pyramid is also orientation dependent. In any sector, trails of abundant fine inclusions (?rutile), here termed type-3 inclusions, may have a single orientation, parallel to type-2 inclusions, or range of orientations, most broadly sub-normal to the pyramid base. Extremely thin, elongate rods, here termed type-4 intergrowths and probably rutile needles, show three predominant, narrowly defined orientations, parallel to the A4 rotational axes, across the whole sector-zoned region. As they do not define sectors, their relation to textural sector-zoning is unclear. Relating natural textural sector-zoning patterns to theoretical patterns was generally difficult, since small, poorly developed core and rim sectors cannot be properly delineated. Textural sector-zoning and matrix displacement microstructures are important criteria for establishing non-kinematic growth events and hence should be actively sought when undertaking tectono-metamorphic studies.

Texturelle Sektor-Zonierung in pelitischen Gesteinen steht mit der Verdrängung von unlöslichen Matrixphasen, vor allem Graphit in Zusammenhang. Dies erfordert eine hohe lithostatische (nicht-differentielle) Spannungskomponente mit hohem Fluiddruck, und ist daher ein Indikator für nicht-kinematisches Mineralwachstum. Theoretische Sektor-Zonierungsmuster in Granat zeigen eine Abhängigkeit der Mikrostrukturen von der Schnittlage und dem Kristallhabitus; Kombinierte rhombendodekaedrische-ikositetraedrische Kristallformen können mindestens 20 Sektoren aufweisen. Im Dünnschliff hängt die Breite der Typ-1 Einschlüsse (Matrix-Einschlüsse) an Sektoren-grenzen von deren Winkel mit der Schnittfläche ab. Auch die Länge der Typ-2 Verwachsungen, die (sub)normal zur Basis der Wachstums-pyramide orientiert sind, ist Schnittlagen-abhängig. Charakteristische Einschlußzüge von sehr feinkörnigen Phasen (?Rutil), die hier als Typ-3 Einschlüsse bezeichnet werden, können in allen Sektoren eine bestimmte Vorzugsorientierung parallel zu Typ-2 Einschlüssen, oder eine Streuung um die Orientierung subnormal zur Basis der Wachstumspyramide aufweisen. Extrem dünne, stark gelängte Leisten (vermutlich Rutil-Nadeln), welche als Typ-4 Verwachsungen bezeichnet werden, weisen im gesamten Sektor-zonierten Bereich drei dominante, sehr eng begrenzte Orientierungsrichtungen parallel zu den A4 Rotationsachsen auf. Da sie keine Sektoren definieren, ist ihre Korrelation mit der texturellen Sektor-Zonierung unklar. Ein Vergleich der beobachteten Muster textureller Sektor-Zonierung von natürlichen Gesteinsproben aus den Alpen mit den theoretischen Mustern war schwierig, da kleine, nur schwach entwickelte Kern- und Randsektoren nicht exakt abgegrenzt werden konnten. Texturelle Sektorzonierung und Matrix-Verdrängungsstrukturen sind wichtige Kriterien für den Nachweis nicht-kinematischer Mineralwachstumsphasen, und sollten daher bei Untersuchungen tektono-metamorpher Prozesse beachtet werden.

1. Introduction

In a simple sketch, Zwart (1962) provided a conceptual basis for determining whether a porphyroblast grew pre-, syn-, or post-tectonically in relation to a foliation. With few controversies (Misch, 1971; Ferguson and Harvey, 1972; Shelley, 1972; Spry, 1972; Bell et al., 1993; Passchier et al., 1993) and no substantial modifications, this scheme has withstood the test of time (Passchier and Trouw, 1996; Vernon, 2004). However, whilst Zwart (1962) noted straight, curved and crenulated inclusion geometries within porphyroblasts, textural sector-patterns were not included, although previously reported (e.g. Harker, 1950; Raisin, 1901).

In this article, textural sector-zoning has been described as inclusion patterns formed both in idealised rhombdodecahedral and icositetrahedral garnets and in natural examples from the Alps. The aim has been to show the wide variations possible in the natural development of textural sector-zoning, from excep-

tionally well through to very poorly developed examples, how it can be recognised and interpreted and what it indicates about the growth history in general.

2. Textural Sector-Zoning and related microstructures

Sector-zoned crystals consist of a number of pyramids, the bases of which correspond to the crystal faces. Where all crystal faces have the same form (and hence the same interfacial energy), all the pyramids meet at the centre of the crystal and theoretically are all the same size and shape (Fig. 1A, C). Each pyramid is thought to have grown as a series of lineages in the form of screw dislocations, oriented essentially normal to the crystal faces, with each lineage being slightly mismatched crystallographically in respect to adjacent lineages (Zwicky, 1929; Buerger, 1934; Petreus, 1978; Burton, 1986).

Two types of inclusions have been documented in textural sector-zoned crystals (Andersen, 1984; Burton, 1986). Type-1 inclusions, which usually occur at growth pyramid margins, and thus reveal the sectoral pattern of the crystal, are derived from the matrix and hence matrix microstructures will be preserved by these inclusions. In cases where a growth pyramid has broken up into discrete growth regions, matrix-derived inclusions may also occur within pyramids, forming inclusion bands normal to the pyramid base, separating growth prongs, (Rice and Mitchell, 1991). Type-2 intergrowths, which are elongate rods of (generally) quartz oriented normal to the crystal faces, grew at the same time as the surrounding porphyroblast.

The observed maximum length of type-2 intergrowths in a growth pyramid varies with the angle between the thin-section and the relevant crystal face (Fig. 2). When the thin-section is parallel to a crystal face, and thus normal to its growth direction, type-2 intergrowths appear as essentially rounded inclusions. When the thin-section is perpendicular to a face, type-2 intergrowths have a maximum dimension constrained only by the size of the pyramid, but may be shorter. Inspec-

tion of the direction of plunge of the type-2 intergrowths reveals whether the porphyroblast centre lies above or below the plane of the thin-section (Fig. 2). Further, the angle of type-2 intergrowths to the plane of the section, determined from their length and the thin-section thickness, can be used to estimate the orientation of the crystal faces relative to the thin-section. In some instances, essentially linear trails of abundant very small inclusions occur parallel to the type-2 intergrowths (Rice and Mitchell, 1991). These trails are here termed type-3 inclusions. Both type-2 intergrowths and type-3 inclusions have been presumed to define lineage boundaries.

A critical distinction proposed by Zwart (1962) is that where a

A) Rhombdo-
decahedron

B) Icositetrahedron-
rhombdodecahedron

C) Icositetra-
hedron

Selected profiles through rhombdodecahedral sector-zoned garnets

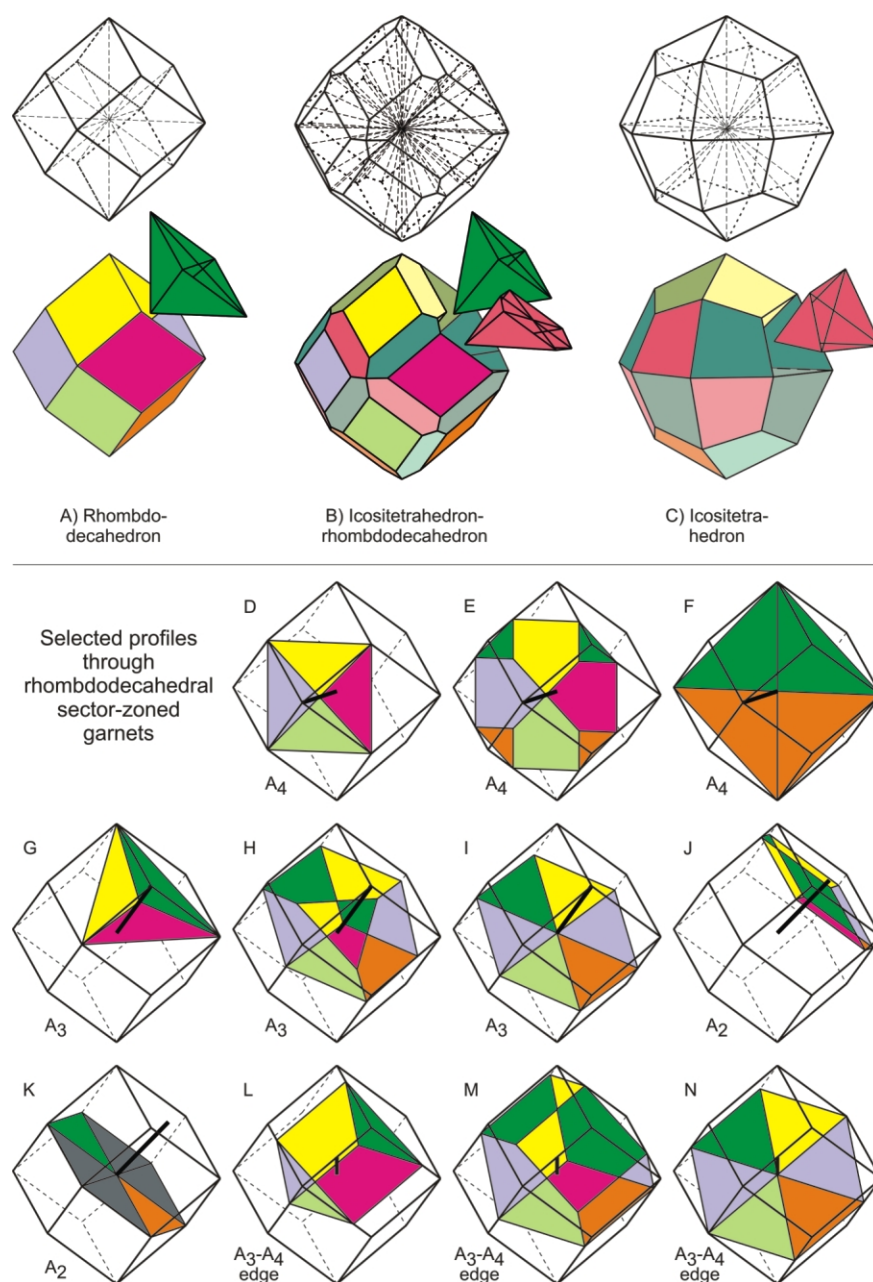**Figure 1:** A, B, C 3-D models of rhombdodecahedral, combined icositetrahedral-rhombdodecahedral and icositetrahedral garnets. One pyramid of each form has been pulled out to show its shape; B-L Selected theoretical symmetrical rhombdodecahedral sector-zoning patterns. See Figs. 1A-C for colour code. The alternating patterns of shading continue around the garnet and have been used in Figs. 1D-N, 3 & 4.

foliation is bent around a porphyroblast, it is presumed that the latter grew earlier than the former. This interpretation differed from some interpretations, which argued that the foliation formed earlier and had been pushed aside and bent by the growing porphyroblast. Misch (1971) re-awakened this suggestion, initiating a discussion on whether crystals can push aside their matrix during growth (Misch, 1971; Ferguson and Harvey, 1972; Shelley, 1972; Spry, 1972). Yardley (1974) critically noted that if a crystal was to push material aside, it would do so in all directions, not just normal to the surrounding foliation, as seen in the classic augen microstructure, and that a crystal would not push aside insoluble or weakly soluble grains whilst overgrowing grains of soluble minerals. Furthermore, Yardley (1974) realised that a crystal displacing its surrounding matrix material does not have to lift the whole rock-pile above it, but has only to exert enough stress to cause dissolution in the directly adjacent volume, into which insoluble material can be displaced. This requires high fluid-pressures, with the stresses exerted by the growing crystal passing through insoluble material at the crystal face to soluble grains slightly further away. As soluble grains are removed, the insoluble grains accumulate 'in' or beside the fluid phase at the edge of the crystal, as it grows. This process is assisted by the volume loss associated with many garnet-forming reactions, due to the higher combined density of the products compared to the reactants, with the creation of a fluid phase. For example, the reaction:

3 anorthite + annite = grossular + almandine + muscovite (Spear, 1993, reaction 17-16)

results in a 17% molar volume loss, whilst the reaction:

2 paragonite + annite + 3 quartz = 2 albite + muscovite + almandine + $2H_2O$ (Spear, 1993, reaction 17-15)

yields a net volume increase of 1%, but if the fluid is excluded, it yields a 6% molar rock-volume decrease (using thermodynamic data from Holland and Powell, 1998).

Using a finite-element model, Ferguson et al. (1980) showed that a crystal growing under a high hydrostatic stress would form a cleavage with an arcuate form (domal in 3-D; cleavage dome) at its margin; this is, essentially, a pressure-solution fabric. Note that hydrostatic stress is here taken to mean lithostatic stress.
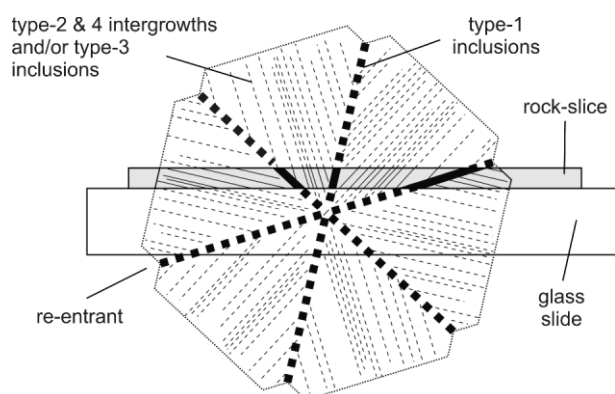
Thus the presence of cleavage domes is not just a sign of displacement growth, but also of a non-differential stress. Essentially, it indicates a non-kinematic growth period. During continued porphyroblast growth, earlier stages of cleavage domes are flattened against the crystal faces, forming a solid, often domal, mass of insoluble material; these are here also included in 'cleavage domes', although no cleavage is present.

In a wide range of minerals, from regional and contact metamorphic environments, as well as from diagenetic and hydrothermal settings, textural sector-zoning was found to have developed in rocks with graphite in the mode and that this had been displaced during growth, although in some cases the textural sector-zoning was poorly developed and the amount of displacement minor (Rice and Mitchell, 1991; Rice, 1993).

As growth occurs normal to crystal faces in texturally sector-zoned crystals (indicated by the type-2 intergrowths), each growth increment results in a small re-entrant at the boundaries between faces. To fill this, growth parallel to the crystal face is required (Andersen, 1984). Where this is not accomplished, the re-entrant will increase in size. Although re-entrants are not commonly seen in garnets (but cf. Rice, 2007), they are frequently found in chiastolite (Rice, 1993). Thus, intuitively, the presence of re-entrants seems to be an indirect sign of (textural) sector-zoning.

3. Textural Sector-Zoning patterns

3.1 Theoretical patterns

Theoretical sectoral patterns for rhombdodecahedral and icositetrahedral garnets (Fig. 1A, C), applicable to chemical, textural and twin sector-zoning, have been constructed, based on the assumption that all pyramids meet at the crystal centre (Figs. 1D-N, 3). For both habits, ideal symmetrical sector patterns have been drawn as profiles oriented either perpendicular to an axis of rotational symmetry or parallel to a crystal face or perpendicular to the plane bisecting two faces along a crystal edge and at the same time parallel to the edge. One set of patterns for mixed rhombdodecahedral-icositetrahedral garnets (Figs. 1B, 4M-S) and two for random orientations through an icositetrahedral garnet have also been constructed (Fig. 4A-L). Three dimensional reconstructions of sector-zoning in other minerals have been presented by Harker (1932), Hollister and Gancarz (1971), Petreus (1978), Kwak (1981), Kouchi et al. (1983), Reeder and Protsky (1985), Cressey et al. (1999) and Bosze and Rakovan (2002).

3-D garnets were created using the Miller indices (cf. Phillips and Phillips, 1980). For the rhombdodecahedral habit, there are three types of rotational axes (A_4, A_3, A_2), where A_2 is normal to the crystal faces, and all edges link A_4 to A_3 axes. For the icositetrahedral habit, there are the same rotational axes but none is face normal and there are two edge types; linking A_3 to A_2 and linking A_4 to A_2. For each orientation, nearly all variations in the sector geometry have been drawn (see http://homepage.univie. ac.at/alexander.hugh.rice); a selection is shown in Figs. 1D-N, 3 and 4; these use the shading in Fig. 1A-C, with colours alternating around the crystal.

Figure 2: Schematic illustration showing the dependence of type-1 inclusion width and type-2 and 4 intergrowth and type-3 inclusion lengths on section orientation.

In thin-sections, broader zones of type-1 inclusions form at lower angled cuts through sector boundaries (Fig. 2). When the section cuts along a sector boundary, thus passing through the crystal centre, it will be filled with inclusions (poikiloblastic) if type-1 inclusions are present. In the icositetrahedra habit, such sections normal to A_3 may be entirely poikiloblastic (Fig. 3C), whilst in sections perpendicular to A_2, only four 'sectors' may be poikiloblastic, in both habits (Figs. 1K and 3H).

Sections through rhombdodecahedra give simpler sector patterns, because there are fewer faces (maximum of nine sectors; Fig. 1H; A_3 symmetry). In the icositetrahedra habit, the maximum is 17 sectors (Fig. 3L; A_2-A_3 edge), representing parts of more than half of the pyramids (24 in all). For both habits, the minimum number of sectors is three, formed (sub-)normal to A_3, close to the crystal rim (Fig. 1G).

The patterns reflect the orientation of the section with respect to the symmetry axes; sections perpendicular to A_3 axes show a threefold rotational symmetry, whilst those perpendicular to A_4 and A_2 axes show four- and two-fold rotational symmetry. The edge sections and the icositetrahedra face-parallel sections show only a single axis of reflection symmetry, with no rotational symmetry, except for sections through the centre of the crystal. The latter show six-fold rotational symmetry for the icositetrahedra A_2-A_4 edge and face-parallel sections and a two-fold rotational symmetry for the icositetrahedral A_2-A_3 edge sections (Figs. 1D-N and 3). The position of the rotational axes can be determined from the sector pattern; for example, the point where three sectors meet is the intersection with a three-fold symmetry axis. In icositetrahedral garnets, both two- and four-fold axes of rotation lie at points where the projection of four faces meet; the two-fold axes are linked along a single face boundary to a three-fold axis, whilst the four-fold axes are not.

Sections cut close to the crystal rim have relatively few sectors, with short, steeply dipping (relative to the plane of the section) type-2/3 intergrowths/inclusions. Sectors can also be identified from the distribution of type-1 inclusions, when present. As the section, whatever its orientation, approaches the centre of the crystal, the number of sector

increases. A group of central sectors (the main sectors in the rim sections) with short and steeply plunging type-2 intergrowths/type-3 inclusions is surrounded by a group of sectors with relatively long and shallowly plunging type-2 intergrowths/type-3 inclusions. All the small sectors disappear when the section cuts through the crystal centre.

Several sections through the garnet centre are parallel to sector boundaries, and thus, in porphyroblasts with abundant type-1 inclusions, will be poikiloblastic (see above). A tectonic fabric within the matrix will be preserved in these sectors. The symmetrical distribution of the poikiloblastic and inclusion-free areas should indicate that textural sector-zoning is present, even when type-2 intergrowths, type-3 inclusions, cleavage domes and re-entrants are absent. Only in the case where all the sectors are filled with inclusions (Fig. 3C) will the sectoral growth pattern be unrecognisable; in such cases, displacement of matrix grains
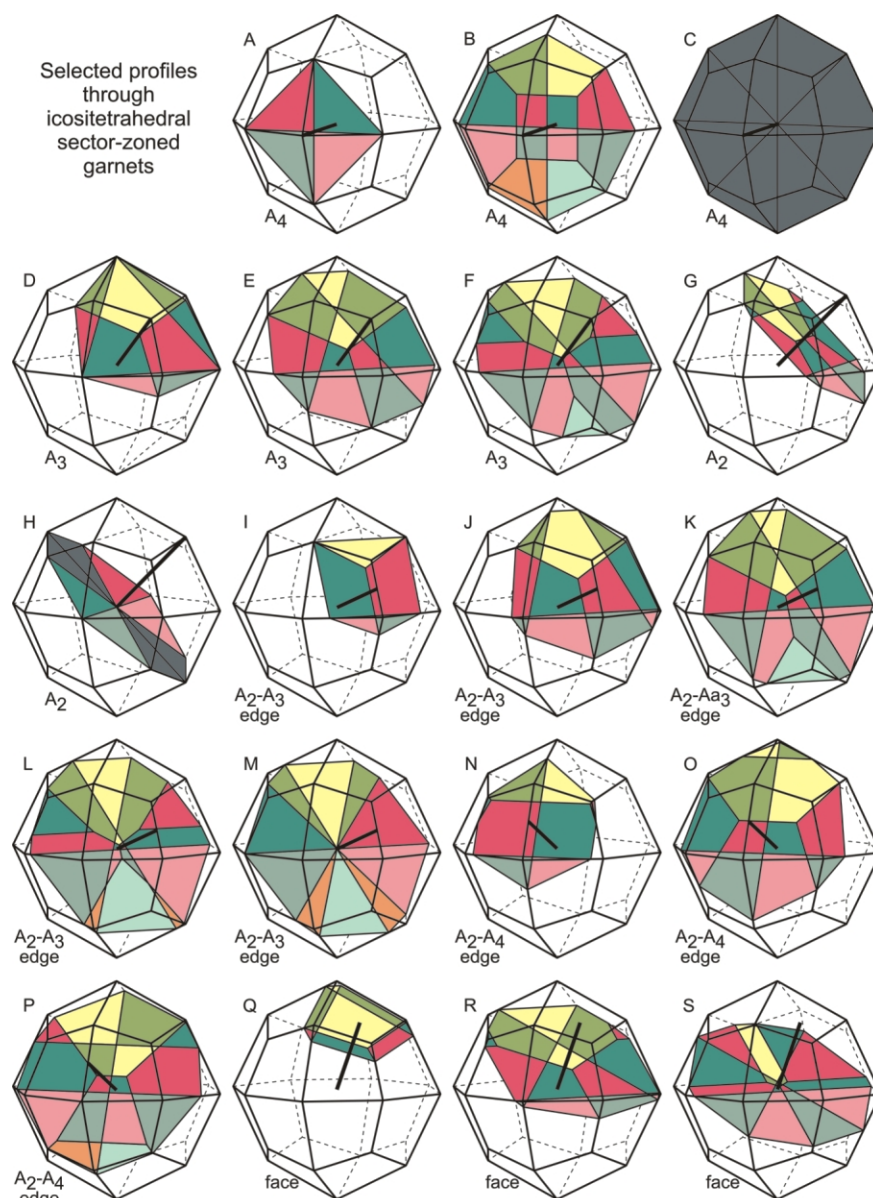

Figure 3: Selected theoretical symmetrical icositetrahedral sector-zoning patterns. See Fig. 1 for colour code.

will also not be noticeable, since this process disappears at the edges between crystal faces, and re-entrants will not be visible.

The patterns in Figs. 1D-N and 3 are symmetrical, although in some cases this is only of a low order. In reality, a thin-section is likely to be oblique to those described, even if it cuts through the centre of a porphyroblast. To evaluate how this would affect the patterns, a sector-zoned icositetrahedral garnet was created in the three-dimensional visualization program GOCAD and sliced at several orientations. The range of possible sector patterns is very large, but all must be mixtures of the previously defined symmetrical patterns; some asymmetric patterns have been shown in Figs. 4A-L.

The above descriptions refer to garnets in which all faces have the same form (here, either {110} or {211}) and thus the same interfacial energy. However, many garnets exhibit intermediate forms, with the edges of the {110} faces variably truncated by {211} faces (or more complex forms). In these instances, all the faces of each form tend to be equally well developed on a single porphyroblast, although this may vary from crystal to crystal in a hand-specimen. Sector patterns in such garnets are complex, since the interfacial energy of the two forms may vary with time, giving curved or irregular sector boundaries. Figs. 4M-S show a series of theoretical profiles perpendicular to A_4 through such a garnet; it has been assumed that the interfacial energies remained constant during growth, so that sectors enlarge outwards at a constant angle. Up to 20 sectors are cut, out of a total of 36, with the number dropping to 4 when the section cuts through the centre, with eight sector boundaries (poikiloblastic areas) also present.

3.2 Natural examples

Texturally sector-zoned garnets are relatively common in the Alps, although rarely referred to (but see Selverstone and Munoz, 1987; fig. 17-38 in Spear, 1993; Leute, 2000; Gauchat and Baumgartner, 2006). For the examples shown here, thin-sections were made parallel to the stretching-lineation and normal to the dominant schistosity and hence are randomly oriented relative to the garnet symmetry axes. The fabric descriptions relate to textural sector-zoning and displacement microstructures; other microstructural aspects are not necessarily covered.

3.2.1 Monte Leone Nappe, Pennine Nappes, High Formazza Valley, Switzerland

The Monte Leone Nappe (Lepontine Alps; Lower Pennine Nappes), was metamorphosed to 550°C at 0.95 GPa during the Neo-Alpine deformation at 29.7-26.7 Ma (Bolli et al., 1980; Vance and O'Nions, 1992; Carrupt, 2002). Within the nappe, the 1-10 m thick, Triassic to mid-Cretaceous graphitic Rifugio Mores Schist (Holzerspitz Series) contains garnetite nodules up to 30 cm long and 5 cm thick, lying parallel to the foliation (Carrupt, 2002, 2003). Garnet porphyroblasts in both the nodules and schists display textural sector-zoning and displacement microstructures, although these vary with the graphite content.
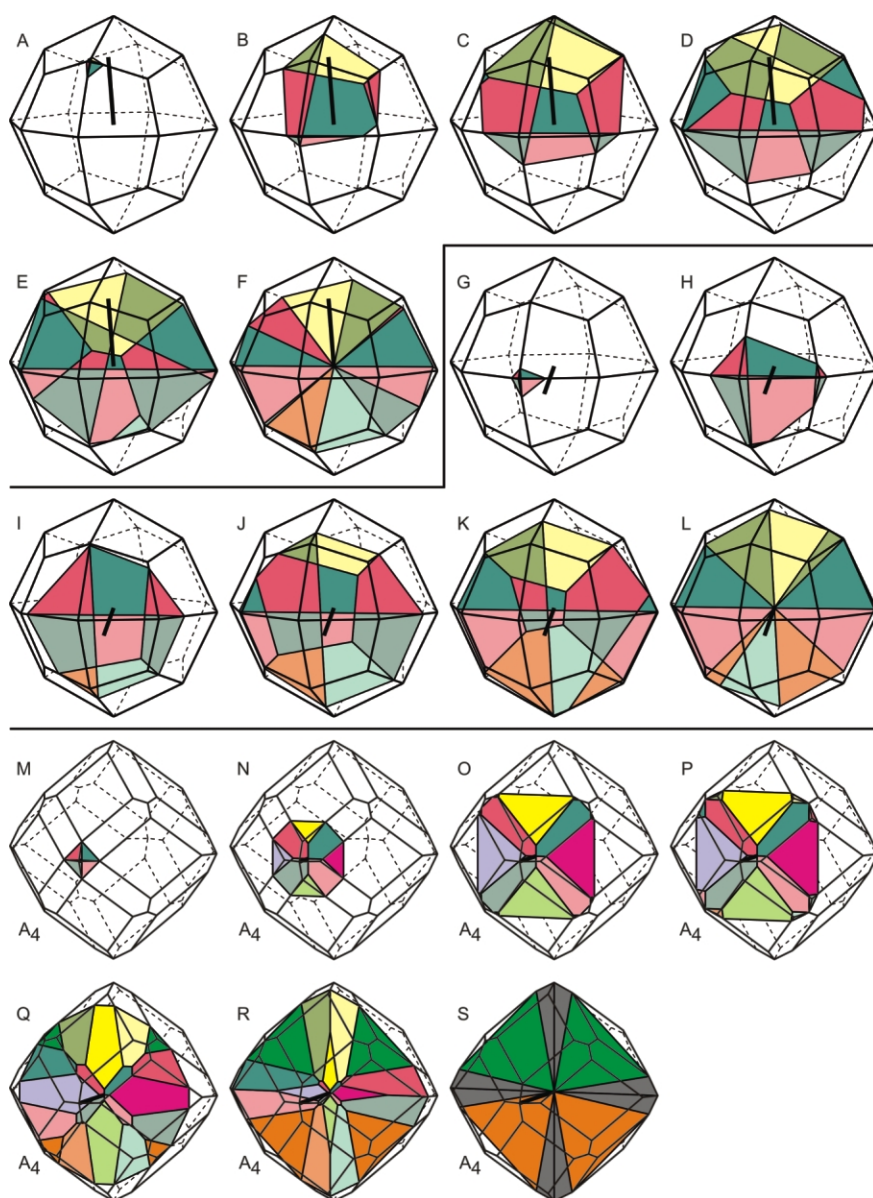
In graphite-poor schists, garnets

Figure 4: Selected theoretical asymmetrical icositetrahedral profiles and profiles through a mixed icositetrahedral-rhombdodecahedral garnet. See Fig. 1 for colour code.

show a sygmoidal inclusion pattern, (<90° rotation relative to the external fabric). Typically, porphyroblasts are ca. 1 mm in diameter, with a xenoblastic inclusion-free core and graphite-richer sub-idioblastic rims. Evidence of textural sector-zoning is poor, coming from arcuate graphite masses that may be cleavage domes (Fig. 5A). However, garnets in sample EC27 (Fig. 5C) are 1.5 cm in diameter, with a poikiloblastic core preserving S3 with S2 microlithons. Small inclusion-free regions contain type-2 intergrowths sub-perpendicular to the adjacent crystal face (Fig. 6B) and have slight arcuate graphite and rutile accumulations (cleavage domes) at their outer ends (Fig. 7A).

In graphite-rich schists, type-2 intergrowths are rare and type-1 inclusions in xenoblastic garnet cores are usually too sparse to show textural sector-zoning (Fig. 8B), but define a planar S3 fabric. Idioblastic to sub-idioblastic garnet rims have abundant graphite and quartz inclusions which may initially pa-

rallel the core S3 fabric but are typically crenulated (S4). The core-rim transition is irregular due both to small, well-defined graphite cleavage domes on growth prongs and to re-entrants which broaden outwards.

The ~5 mm thick nodule rims have high graphite contents (C_{org} <95%; Carrupt, 2002), with garnet and minor quartz and chlorite. Garnet cores are up to 1.4 mm in diameter, (sub-)idioblastic, and essentially inclusion free except for fine type-1 inclusions defining feather-edged textural sector boundaries, which may broaden outwards slightly to small re-entrants. No preferred orientation is preserved in these type-1 inclusions. A few type-2 intergrowths and fine inclusion bands are present. When conditions for displacement growth ceased, the displaced graphite inhibited further growth, which was restricted to sector boundaries or re-entrants, where little or no graphite displacement occurred. This phase of growth was poikiloblastic and, once past
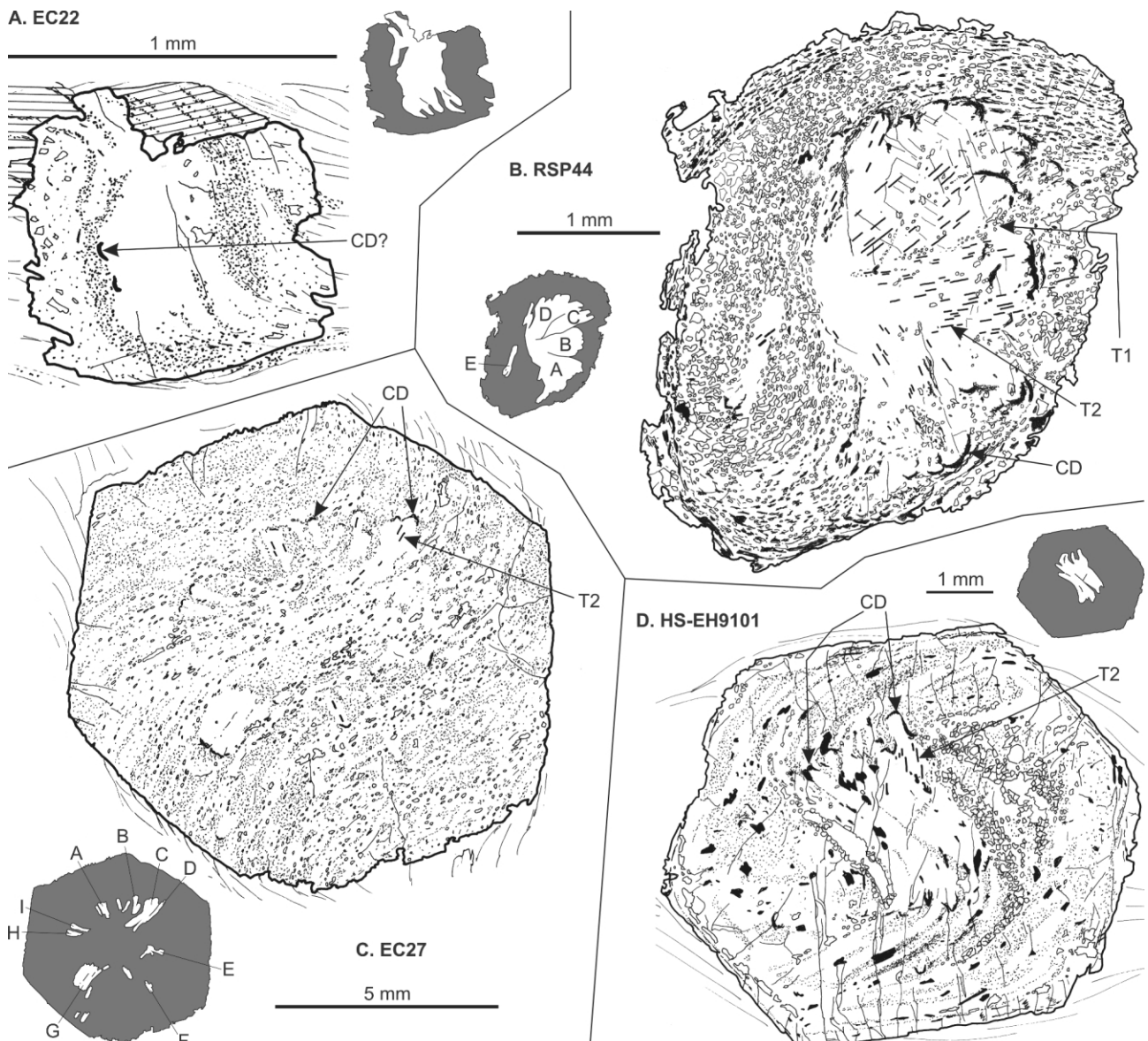

FIGURE 5: Sketches of spiral garnets with some evidence of textural sector-zoning. CD – cleavage dome; IB – inclusion band; RE – re-entrant; T1 – type-1 inclusions; T2 – type-2 intergrowths; T3 – type-3 inclusions; T4 – type-4 intergrowths; ky/sill – kyanite/sillimanite inclusions; CF – 'cauliflower' growth.

the band of displaced graphite, it broadened out, gradually overgrowing the band of displaced graphite, with a form like a cauliflower (Carrupt, 2003; Fig. 7B), ultimately merging with growth from adjacent sector boundaries. Where the rim mineralogy was less graphitic, microstructural development was comparable to that in the matrix surrounding the nodules. Fig. 8A shows a porphyroblast which lies at the edge of the nodule rim; one half has microstructures typical of the nodule-rim garnets, the other has microstructures similar to garnets in the graphite-rich matrix (cf Fig. 8B).

Garnet is the dominant phase in nodule cores, with graphite (C_{org} 0.8% to 4.7%), quartz, chlorite, opaque minerals and rare biotite as minor interstitial phases. Garnets are <0.4 mm in diameter, and often show partial idioblastic shapes but, due to the high nucleation density, they have impinged on each other, inhibiting growth (Fig. 8C). Three microstructural growth zones occur, the first two represent cycles of matrix overgrowth followed by displacement. The first (sub-idioblastic) zone contains abundant randomly oriented fine inclusions of graphite and white mica in the core. The inclusion density decreases towards the zone edge, with some type-1 inclusions defining sector boundaries. The second zone initially comprises massive graphite in a curved band up to 0.05 mm thick, interpreted as material displaced from the first zone. Outside this is a zone of abundant, evenly dispersed and oriented graphite, which decreases in abundance, indicating the onset of displacement growth and textural sector-zoning again. Type-1 inclusions form inclusion bands or define sector boundaries, which broaden outwards and pass into re-entrants. Near the rim zone, a 0.01 mm thick band of graphite may reflect partial interruption in the displacement process. Massive displaced graphite marks the porphyroblast rim, although 'cauliflower structures', as described above have developed in some places (Zone 3). The no-

dules were heavily fractured after the second microstructural zone, with numerous quartz-filled cracks forming around the garnets. This was then skeletally overgrown by a thin graphite-free garnet growth, possibly contemporary with Zone 3.

3.2.2 Rappold Complex, Austroalpine basement, Schöttelbach Valley, Austria

Sample RS/WÖ18/2000-HR is from the Rappold Complex near Großhansl, in the Schöttelbach valley in Styria, Austria. This unit comprises paragneisses with graphitic garnet-staurolite-micaschists, from which the sample was taken, and thick marble layers and minor amphibolites. Three metamorphic events occurred; a presumed Variscan event at ca. 535 °C/0.54 GPa is defined by medium- to high-pressure mineral assemblages (garnet + staurolite + kyanite; Gaides et al., 2006). Sm-Nd garnet isochron ages indicate Permian pegmatite intrusion at 288 ± 4 Ma and 262 ± 2 Ma (Schuster et al. 2001), contemporary with andalusite growth, reflecting a low-pressure overprint. The youngest assemblage, of Eo-Alpine age (ca. 85 Ma), led to kyanite replacing andalusite and garnet growth at existing porphyroblast rims and new nucleation sites, at ca. 625 °C and 1.1 GPa (Schuster et al., 1999, 2004; Thöni, 1999; Faryad and Hoinkes, 2003).

Garnet porphyroblasts show three microstructural zones (Fig. 9C). The central and largest zone seems to be inclusion free apart from a few large opaque inclusions. However, closer examination reveals pervasive type-3 inclusion trails, 0.0025 mm apart, with inclusions 0.0008 mm across, defining textural sector-zoning, with relatively rare type-2 intergrowths (Fig. 6E) parallel to adjacent type-3 inclusions. The rim of this zone is marked by irregularly spaced cleavage domes (Fig. 7C), defining a sub-idioblastic outline, cutting into a relict compositional banding preserved within zone 2 and either wrapped around
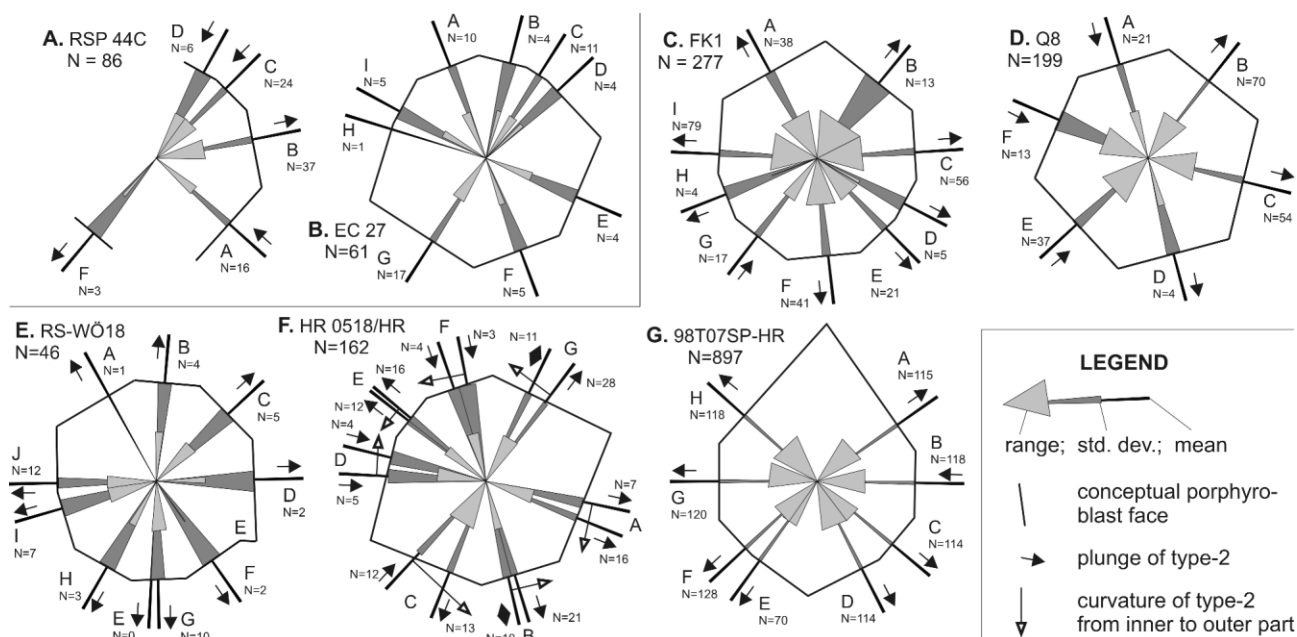

Figure 6: Rose diagram of type-2 intergrowth orientations.

the core or cut across by the latter. Locally, the type-3 inclusion trails persist a very short distance across this compositional banding. The outer zone is xenomorphic, reflecting a new nucleation event, with elongate opaque inclusions defining a fabric wrapped around zone 2.

The orientation of the type-3 inclusions, indicating nine sectors around a small central sector, requires an icositetrahedral habit. The central sector has very short type-3 inclusions, showing that they lie at a high angle to the plane of the thin-section, but these cannot be reliably sub-divided. However, as it appears to have a pentagonal shape it may have five sectors, although this has not been seen in any theoretical pattern.

3.2.3 Venediger Nappe, Tauern Window, Maurer Valley, Austria

Sample FK1 comes from Carboniferous fossil plant-bearing graphitic schists in the Maurer Valley, overlying para- and orthogneisses of the Venediger Nappe, in the Tauern Window (Pestal et al., 1999). Idiomorphic almandine porphyroblasts up to 10 mm in diameter formed under growth conditions changing from ca. 400-450°C (core) to 500-550°C/0.75 GPa (rim; Koller in Pestal et al., 1999) in an Alpine event dated at ~35-30 Ma (Frank et al., 1987). The porphyroblasts are wrapped by a crenulated, graphite-rich pelitic foliation.

Garnets (Fig. 9A) have few type-1 inclusions (quartz, carbonate and opaques), which do not define any fabric, and abundant short, very fine (0.008 mm thick) quartz type-2 intergrowths, (sub-)normal to the adjacent crystal face and defining a textural sector-zoning pattern (Fig. 6C). The latter indicate that the sparse type-1 inclusions lie on sector boundaries. The distribution of the type-1 inclusions and type-2 intergrowths shows that nine sectors are present at the porphyroblast rim, indicating an icositetrahedral habit. Although sector H is small, with only a minor difference in type-2 intergrowth trend compared to sector G (Fig. 6C), the opposing type-2 intergrowth plunge

directions confirms that these are different sectors. The intergrowths in sectors D and E are also sub-parallel (Fig. 6C) but these plunge in the same direction; the existence of sector D is thus rather uncertain, but its presence, comparable to sector H, makes the sector pattern symmetrical. In the porphyroblast centre, several minor sectors are defined by opaque type-1 inclusions and occasional type-2 intergrowths. Although the overall sector pattern cannot be fully determined, due to the
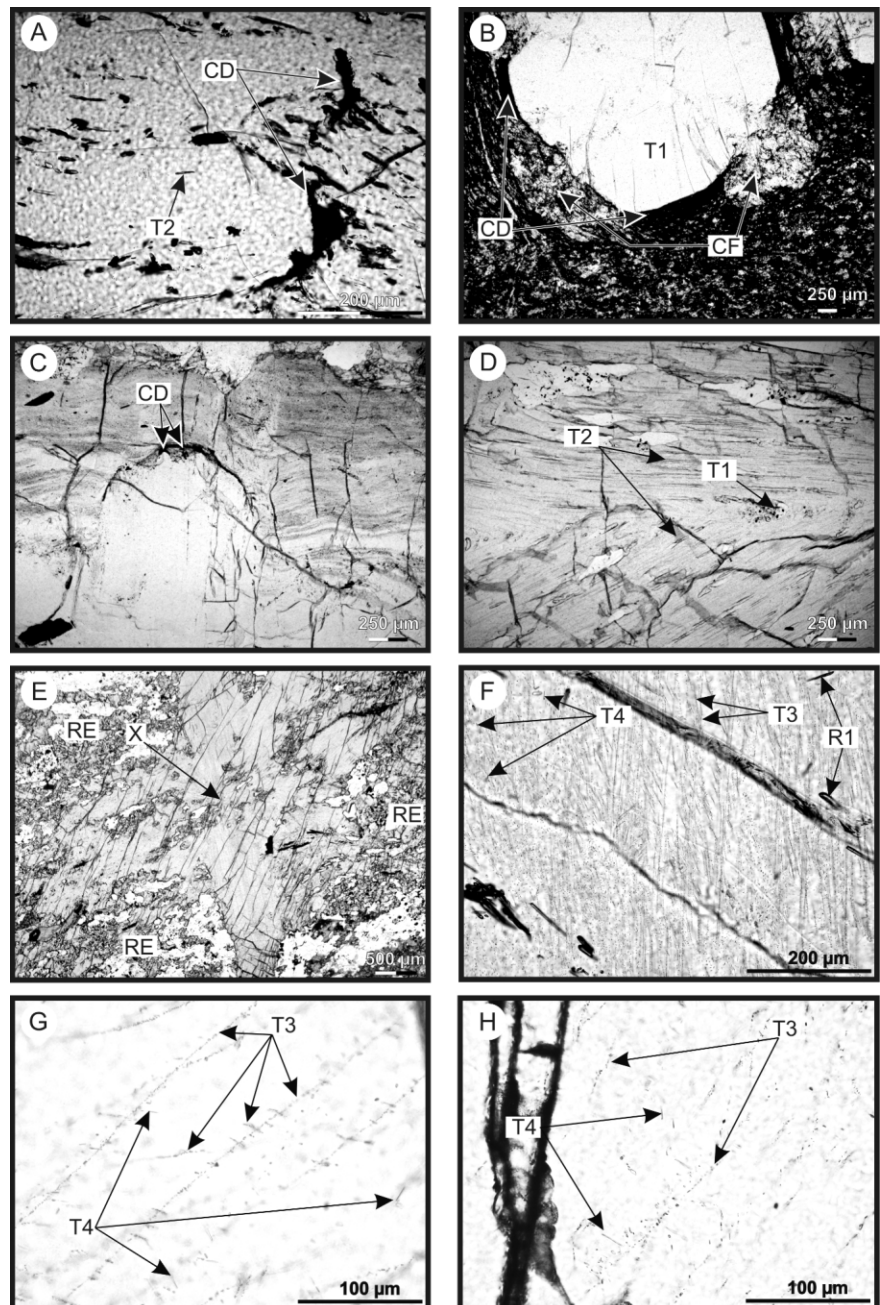
Figure 7: Photographs: A EC1 (similar to EC27) – rutile and graphite dust forming a cleavage dome; B EC111 – showing a 'cauliflower' structures growing from between cleavage domes; C RS-WÖ18 – cleavage dome cutting graphite layering in outer garnet growth zone; D 98T0758 – different orientations of type-2 intergrowths across a sector boundary, one set sub-parallel to the boundary one oblique; E – Q8 type-3 inclusions meeting at the porphyroblast centre (marked X); F – GC1905 multiple directions of type-3 inclusions and type-4 intergrowths; G – GC1905 – rapid changes in orientation and different levels of type-3 inclusions and very short branching out. H 03R52b – curvilinear type-3 inclusions and two directions of type-4 intergrowths.

paucity of inclusions and intergrowths, the general dip of type-2 intergrowths away from the porphyroblast core indicates the centre of the crystal lies above the plane of the section (see Fig. 2).

3.2.4 Gneiss Unit, Austroalpine basement, Saualpe, Austria

Sample GHQ8-H comes from the structurally highest part of the Gneiss Unit, in the Austroalpine Saualpe crystalline basement, which comprises paragneisses, eclogite-amphibolites, calcsilicates and pegmatite mylonites. The sample location lies ca. 200 m below the amphibolite-facies Plankogel Micaschist Unit, in the NW Saualpe, about 2.5 km east of Knappenberg. The Gneiss Unit underwent pre-Cretaceous regional low-pressure/medium to high-temperature metamorphism (ca. 600 °C at 0.4 GPa in garnet cores), thought to correlate with Permo-Triassic extension (Habler and Thöni, 2001; Thöni and Miller,

2000). An Eo-Alpine pressure-dominated overprint reached 1.3 ± 0.2 GPa at 600 ± 30°C. Tectonically intercalated eclogites and their metapelitic host-rock indicate metamorphism at 1.9 ± 0.2 GPa at 690 ± 50 °C (Habler and Thöni, 1998; Thöni and Miller, 1996; Miller et al. 2005).

The garnet studied (Fig. 9B), which comes from a graphitic calc-silicate assemblage, comprises one growth zone, with three microstructural types. The central part has abundant type-3 inclusion trails and type-2 intergrowths (Fig. 9D) diverging in six directions from a single point, indicating that the section cuts through the porphyroblast centre (Fig. 8E), with occasional type-1 quartz inclusions along sector boundaries and forming inclusion bands within sectors. Further from the centre, type-3 inclusions are less common or absent, although type-2 intergrowths are present and still further out, the garnet has a poikiloblastic microstructure with abundant quartz inclusions and scattered

A. EC111A-HR

CD

RE

T1

CF   CD

C. EC253

1 mm

B. EC97

1 mm

CD   RE

IB   CD

T1
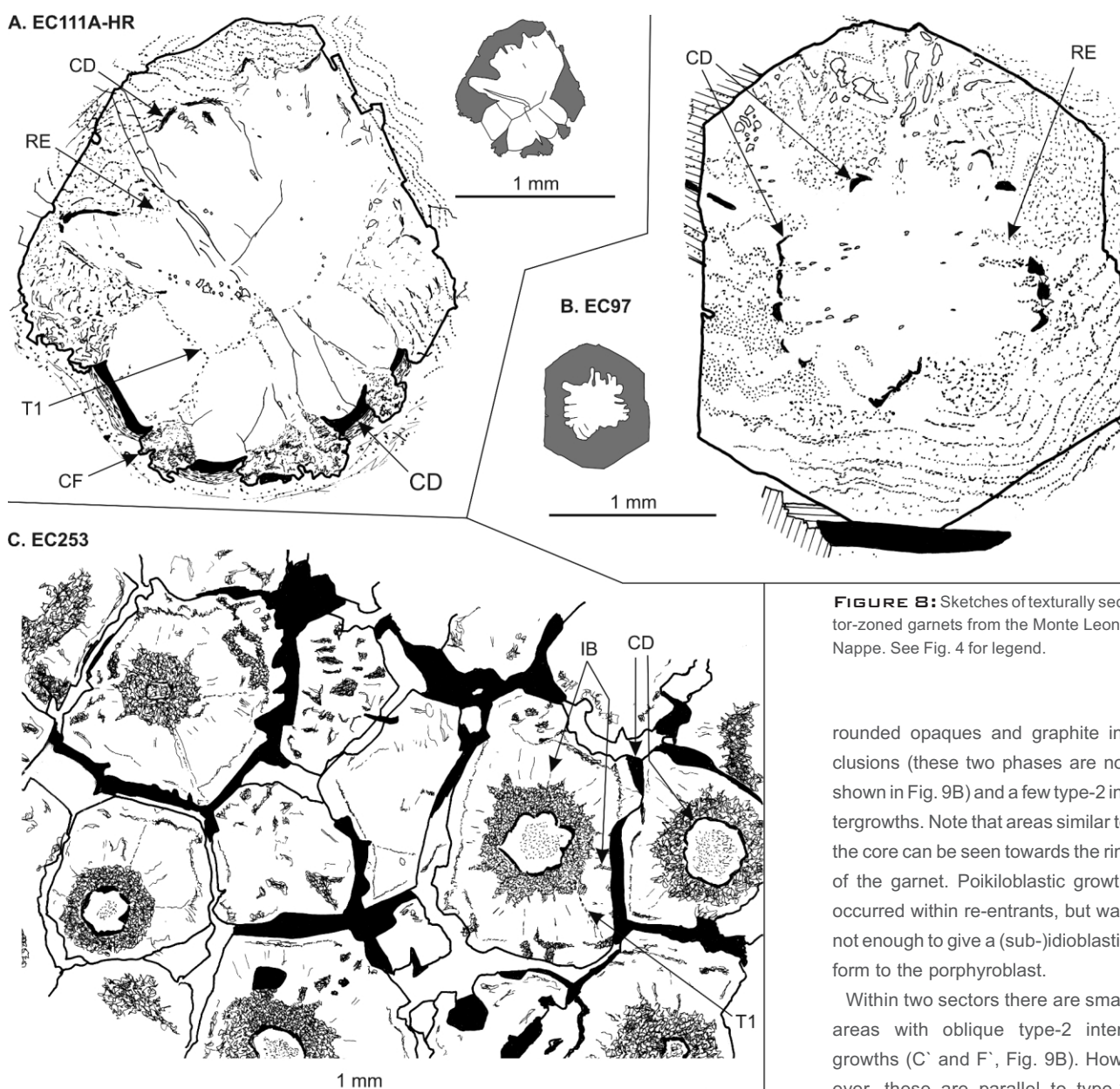
Figure 8: Sketches of texturally sector-zoned garnets from the Monte Leone Nappe. See Fig. 4 for legend.

rounded opaques and graphite inclusions (these two phases are not shown in Fig. 9B) and a few type-2 intergrowths. Note that areas similar to the core can be seen towards the rim of the garnet. Poikiloblastic growth occurred within re-entrants, but was not enough to give a (sub-)idioblastic form to the porphyroblast.

Within two sectors there are small areas with oblique type-2 intergrowths (C` and F`, Fig. 9B). However, these are parallel to type-2
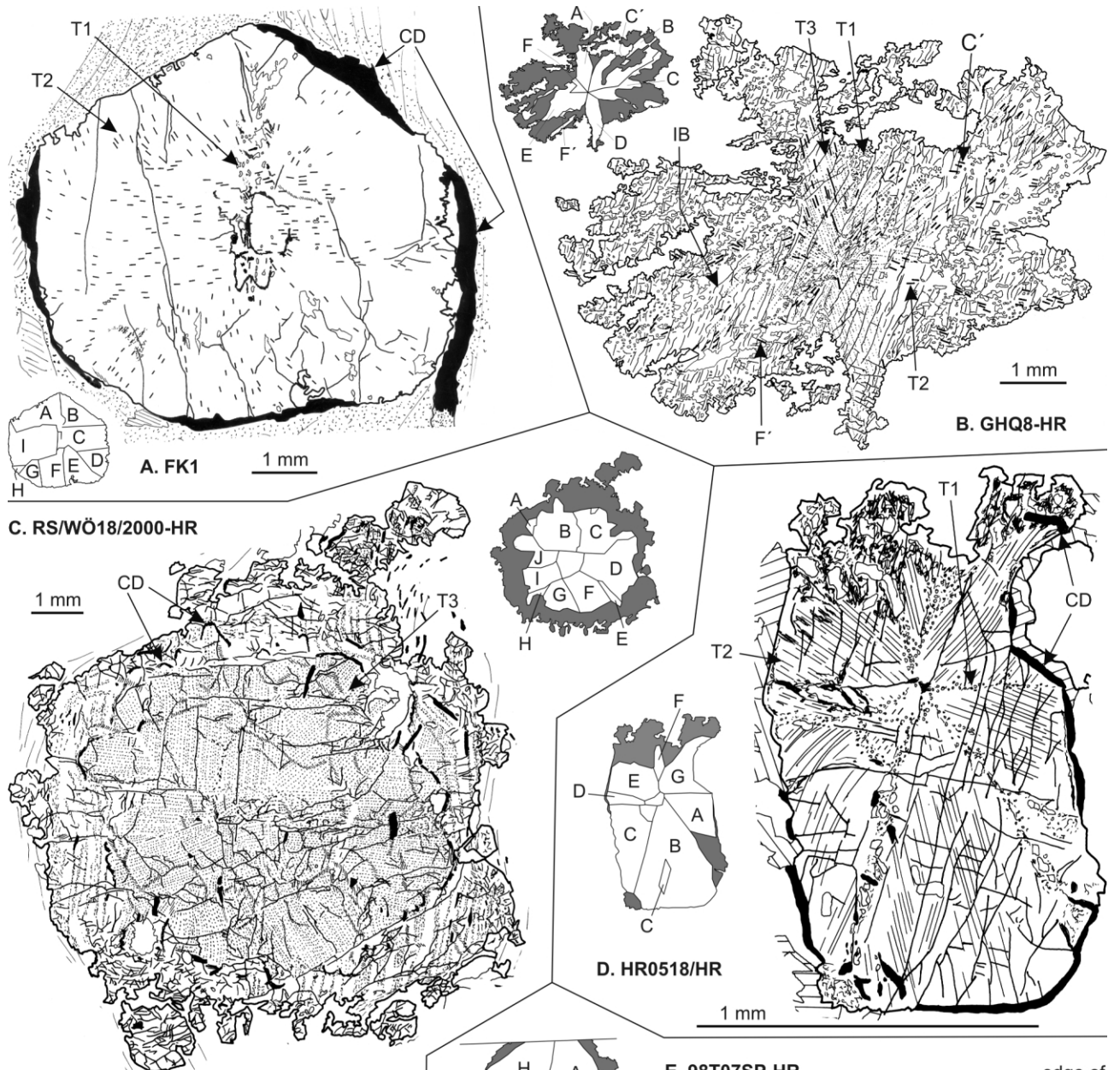
FIGURE 9: Sketches of texturally sector-zoned garnets. See Fig. 4 for legend.

intergrowths in adjacent sectors (sectors C and F) and represent growth coming from the side of growth prongs before poikiloblastic growth occurred forming the nearby inclusion bands. Competing growth directions also resulted in the limited development of sector F in the plane of the section.

In sectors E, F, B and C the intergrowths dip towards the left in Fig. 9C, whilst intergrowths in sectors A and D dip towards the bottom of the figure. The six-fold symmetry indicates a rhombdodecahedral growth habit either viewed down one of the A_3 axes or parallel to a crystal face or perpendicular to a crystal edge (Fig. 1H, J, M). The second option gives four poikiloblastic sectors without any type-2 intergrowths or type-3 inclusions. The other two
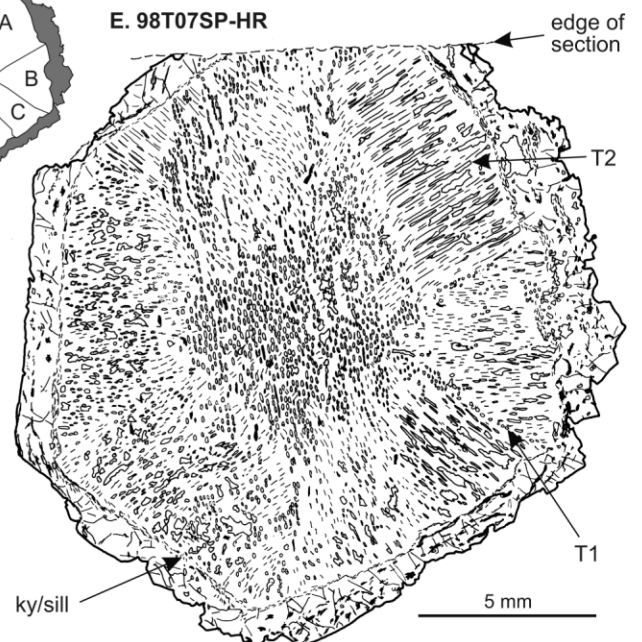
possibilities can be distinguished by the dip of the type-2 inter-growths. In the first scenario, intergrowths in all sectors should be parallel to the plane of the section but not in the second, whilst in the third (or in any orientation between the first and third pos-sibility) the intergrowths in four sectors should plunge through the section and the other two be parallel to the section plane. Since none of these criteria are fulfilled, with all the type-2 inter-growths oblique to the section plane, an orientation somewhere close to the A_3 axes is most probable.

3.2.5 Plankogel Micaschist Unit, Austro-alpine basement, Plankogel and Soboth, Austria

Samples 98T07SP and 03R52b, from the Plankogel Unit (Plan-kogelserie) in southern Austria, were collected close to the sum-mit of Plankogel, near Hüttenberg, in the Saualpe, and from the southern side of Jankitzkogel, near Soboth, in the Koralpe, re-spectively. This complex comprises polymetamorphic garnet-staurolite-mica schists and Mn-rich quartzites, marbles, meta-ultrabasites, amphibolites and rarely meta-pegmatites. Garnet cores yielded Permian Sm-Nd ages between 262 ± 4 and 285 ± 4 Ma (Thöni, 2002 and unpubl. data), constraining the age of the first, prograde amphibolite-facies low-pressure (andalusite-for-ming) metamorphism. A younger assemblage, including garnet, staurolite and chloritoid formed at 550-560°C and 1.0-1.1 GPa in the Koralpe and is presumed to be of Eo-Alpine age (Gregurek et al., 1997). Fine grained kyanite aggregates in this assemblage may have been derived from Permian andalusite during this event. The younger garnet both formed rims around the earlier garnet porphyroblasts and nucleated at new growth centres.

Garnet porphyroblasts in sample 98T07SP are up to 17 mm in diameter, with two main microstructural zones (Fig. 9E). The central zone has a poikiloblastic core, comprising alternating quartz-rich and quartz-poor/graphite-rich layers, derived from overgrowth of the matrix foliation. Areas with no matrix inclusions in this region generally have type-2 intergrowths and sub-parallel type-3 inclusions. As the inclusion density in the poikiloblastic core decreases, type-2 intergrowths and type-3 inclusion trails become ubiquitous, defining eight sectors (Fig. 6G); in some, the type-2 intergrowths became coarser (up to 0.25 mm thick) as they grew. Although sector boundaries are typically indicated by variations in orientation of intergrowths or by type-1 inclusions, the boundaries between sectors C and D, and E and F (Fig. 9E) have been inferred from differences in intergrowth lengths. Type-2 intergrowths are in some cases essentially parallel and in other cases at a high angle to the adjacent sector boundary (Fig. 7D and 9E); this geometry is indicated by some idealised profiles (e.g. Fig. 3F, I, L, S).

The boundary with the outer growth zone is gradual. Type-2 intergrowths and type-3 inclusions end on an irregular margin, leaving a 0.24-0.5 mm inclusion free zone. This is followed by an equally narrow zone in which occasional sillimanite needles are present and then by an up to 0.5 mm thick zone of kyanite/ sillimanite with quartz and ilmenite. The outermost part (0.7 mm wide) comprises numerous small sub-idioblastic garnets, repre-senting multiple nucleations, giving an irregular crystal faces to an essentially idioblastic form; these have irregularly shaped and distributed ilmenite inclusions.

The garnet in sample 03R52b (Fig. 10A) is 1.3 cm in diame-ter and has essentially the same growth zonation as sample 98T0758. The central zone is 1.2 mm in diameter and idiomor-phic, whilst the outer, heavily fractured zone comprises an inner
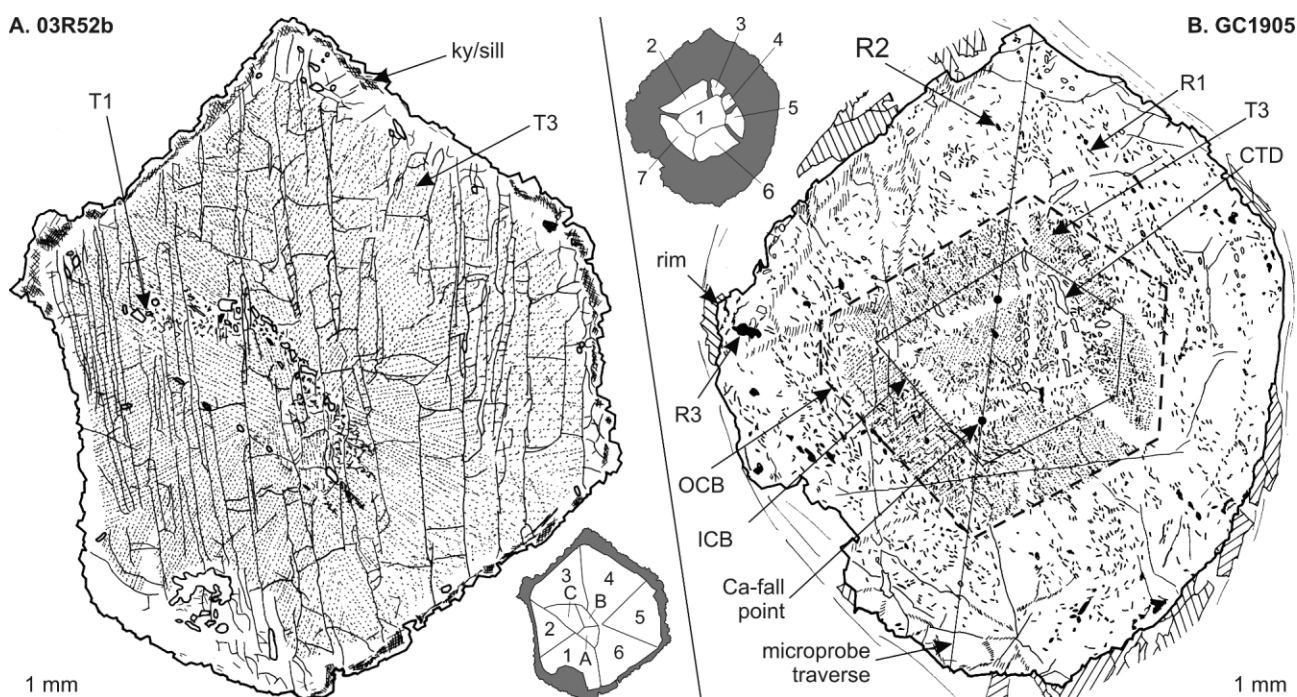

Figure 10: Sketches of texturally sector-zoned garnets with type-4 inclusions. See Fig. 4 for legend. CTD – chloritoid/staurolite inclusions; R1, R2, R3 – Fe-Ti oxide populations; rim – rim growth.

segment with abundant small irregular sillimanite and kyanite laths and an outer inclusion-free segment.

The inclusion pattern indicates that nine pyramids have been cut through (Fig. 10A), with type-1 inclusions bounding six outer and three inner sectors. As the latter are relatively small, the section must lie close to the crystal centre. Three distinct populations of thin (~0.0013 mm wide) elongate inclusions of probably quartz occur (Fig. 7H), each having an extremely narrow range of orientations (Fig. 11 C and F, Table 1). These lie at ~120° to each other, parallel to the boundaries of the outer sectors and plunging towards alternating corners of the garnet. The plunge direction of each orientation is constant throughout the inner and outer sectors. In this, they differ markedly from type-2 intergrowths (cf Burton, 1986) and hence are here termed type-4 intergrowths. No type-2 intergrowths have been observed.

Type-3 inclusions are abundant and show a range of orientations within each sector. The trails are spaced at 0.075 mm or more apart and are formed of irregular inclusions up to 0.013 mm across. In sectors one to three, the commonest orientation is sub-normal to the pyramid base (crystal face), although the curvature of the trails has resulted in a relatively wide range of orientations. Similarly, the inner parts of sectors four to six show a dominant orientation sub-perpendicular to the pyramid base (Fig. 10A). However, the outer parts of the latter three sectors show two dominant orientations, neither of which is either necessarily parallel to the type-3 inclusions in the inner part or perpendicular to the pyramid base. It seems unlikely that the inner and outer parts are separate sectors, since this pattern is not seen in the theoretical patterns.

In some cases, a type-3 inclusion trail may change direction abruptly, but this is not necessarily seen in adjacent type-3 inclusions and differing orientations pass over each other. Most sectors also have some type-3 trails parallel to, and plunging in the same direction as the three type-4 intergrowth orientations.

The hexagonal form, with six outer sectors and three inner sectors, suggests the section was cut sub-perpendicular to A_3 (Fig. 1H). Note that in this orientation, the three A_4 axes lie with at an apparent angle of ca. 120° to each other, plunging parallel to

sector boundaries and towards alternating crystal corners, a geometry matching the type-4 intergrowths.

3.2.6 Radenthein (Wölz) Complex, Austroalpine basement, Predlitz, Austria

Sample RSP44 comes from the Radenthein (Wölz) Complex in the Austroalpine unit east of the Tauern Window, near Predlitz, Styria. This complex is comparable to the Schneeberg Complex, with garnet paragonite schists, amphibolites, marbles and calcareous mica-schists. Peak Eo-Alpine metamorphic conditions were estimated to have been ca. 0.7 GPa at ca. 570 °C (Schuster and Frank, 2000).

The sample is a crenulated graphitic muscovite-biotite-garnet schist with minor kyanite and staurolite. Sub-idioblastic garnet porphyroblasts (4 mm in diameter) show 120° curvature of S_i, with variably developed textural sector-zoning (Fig. 5B). A xenoblastic central zone is essentially inclusion-free, although patches of type-1 inclusions, some along sector boundaries preserve a planar S_i fabric. Quartz type-2 intergrowths indicate four textural sector-zones preferentially developed on one side of the porphyroblast, with one (sector E), isolated from the others, on the other side (Fig. 6A). The core zone either passes directly into a poikiloblastic zone of quartz/opaque inclusions, showing a curved Si fabric, or into arcuate graphitic cleavage domes essentially normal to the type-2 intergrowths. The porphyroblast rim preserves an opaque inclusion fabric partially derived from the strain-caps.

3.2.7 Schneeberg Complex, Austroalpine basement, Valle del Lago, Merano, Italy.

Sample HS-EH9101 was taken from the Bunte Randserie near Merano, in the Valle del Lago, towards the southern border of the western Austroalpine basement realm. The Bunte Randserie, which lies at the outer part of the Schneeberg Normal Fault Zone, is an Eo-Alpine ductile shear zone which exhumed high-pressure metamorphic rocks (Sölva et al., 2005; Habler et al. 2006). This comprises pelitic schists, amphibolites, marbles and calc-schists in layers up to 200 m thick. The main fabric formed

Outer sectors							**Inner sectors**						
Rose	Sector	T3/T4	Mean°	N	Cone°	Max %	Rose	Sector	T3/T4	Mean°	N	Cone°	Max %
a	1	T3	203	59	2	51	p	A	T3	111	26	6	27
b	2	T3	257	74	2	47	p	A, C	T3	113	59	3	34
c	3	T3	332	68	2	65	p	C	T3	114	33	3	52
d	4	T3	025	57	2	60	q	B	T3	151	29	3	38
e	5	T3	072	61	2	44	r	A, B, C	T3	343	8	6	50
f	6	T3	141	27	3	48	s	A, B, C	T3	357	2	11	100
g	1-6	T3	225	147	2	27	t	A, B, C	T3	108	6	7	83
h	1-6	T3	255	2	11	100	u	A, B, C	T3	124	8	6	63
i	1-6	T3	352	134	3	22	v	A, B, C	T3	137	22	3	36
j	1-6	T3	097	35	3	46	w	A, B, C	T3	148	8	6	75
k	1-6	T3	110	114	2	44	x	A, B, C	T4	226	26	3	64
l	1-6	T3	131	79	2	46	y	A, B, C	T4	348	22	3	62
m	1-6	T4	226	182	1	83	z	A, B, C	T4	113	26	3	77
n	1-6	T4	348	164	1	76							
o	1-6	T4	112	180	1	79			Total N = 1,658				

Table 1: Distribution of type-2 intergrowths and type-3 inclusions in sample 03R52b.

during exhumation and was folded by F1 (Sölva et al., 2005) at amphibolite facies (0.8-1.0 GPa, 550-600 °C (Konzett and Hoinkes, 1996). F2 occurred during decompression at amphibolite-facies conditions (Habler, 2004). Garnet cores grew synkinematically close to P_{max} whilst the rim overgrew the mylonitic foliation during and after F2.

Garnets are idioblastic, up to 1 mm in diameter and have a sygmoidal inclusion fabric indicating ca. 115° rotation of the inclusion fabric within the porphyroblasts relative to the external foliation (Fig. 5D). An essentially inclusion free and elongate central zone is bounded at the ends by curved masses of graphite, here taken to be cleavage domes; one of these is associated with a few type-2 quartz intergrowths. This central zone is bound on the sides by quartz inclusion-rich layers which link with a graphite-rich and -poor layering and form the curved S_i fabric. These are taken to reflect an early compositional layering. Abundant quartz inclusions on the right side of the porphyroblast reflect overgrowth of a quartz-rich strain shadow. An outer idioblastic rim (0.25 mm wide), sometimes separated from the core by a thin layer of quartz inclusions and often with thin graphitic layers, represents a later growth around the whole porphyroblast.

3.2.8 Kreuzeck Group, Austroalpine basement, Gursgental, Lienz, Austria

Sample HR0518-HR comes from the western Kreuzeckgrup-pe, which comprises Austroalpine basement, in the Gursgental region south of the Tauern Window. The area underwent Variscan upper greenschist to lower amphibolite-facies metamorphism, forming garnet, biotite, chlorite ± chloritoid-bearing assemblages. Garnet overgrew an axial plane foliation with subsequent major deformation at lower metamorphic grades. Permian metamorphism and pegmatite-emplacement in the eastern Kreuzeckgruppe (Schuster et al., 2001) may not have exceeded greenschist-facies in the sample area, which was only weakly affected by Eo-Alpine metamorphism, at lower greenschist facies conditions.

The sample is a plagioclase-rich mica schist within which some garnet nuclei formed close together in bands 3 mm thick and 15 mm long, such that they intergrew. Subsequent boudinage broke-up the garnet-rich layer, with quartz and chlorite filling the necks; consequently, the outer garnet growth zone is often missing. The texturally sector-zoned xenoblastic garnet cores are up to 2.5 mm across, with 0.4 mm thick poikiloblastic rims, overgrowing displaced graphite and the matrix foliation. The example illustrated (Fig. 9D) has seven outer sectors, all with type-2 intergrowths, several of which are unusually thick (0.04 mm) and long. The latter indicates that the thin-section is perpendicular to the adjacent crystal faces. The type-2 intergrowths are curved, although in sectors B and G the intergrowths curve one way and then back again to their original orientation and in sectors D, E and F the curvature is very slight. In Fig. 6F the type-2 intergrowth orientations in the inner and outer parts of the sectors have been plotted separately, with an arrow showing the sense of curvature.

Sector boundaries are marked by type-1 inclusions of opaques, graphite dust, small quartz grains and larger, irregular epidote group minerals. These define a small central zone containing at least two sectors, with very short type-2 intergrowths, but this cannot be further divided. A thick opaque band around much of the garnet attests to displacement of the matrix graphite (Fig. 9D).

3.2.9 Ötztal-Stubai basement, Pfossental, Merano, Italy

Sample GC 1905 comes from schists in the southern Ötztal-Stubai basement, towards the western margin of the Schneeberg Zug, near Merano, in South Tirol. The sample was taken from the hanging- (west) wall of the up to 5 km thick Schneeberg Normal Fault Zone, separating

A. Main orientation of type-3 inclusions in each outer sector (numbered 1-6). Plunge direction is shown by the arrow.

B. Orientation of type-3 inclusions oblique to the main orientation of the sector they lie in. Combined from all outer sectors. Showing the plunge direction.

C. Orientation of type-4 intergrowths combined from all outer sectors. Showing the plunge direction

D. Main orientation of type-3 inclusions in each inner sector. Sectors A & C are combined. Showing the plunge direction.

E. Orientation of type-3 inclusions oblique to the main orientation of the sector they lie in. Combined from all inner sectors. Showing the plunge direction.

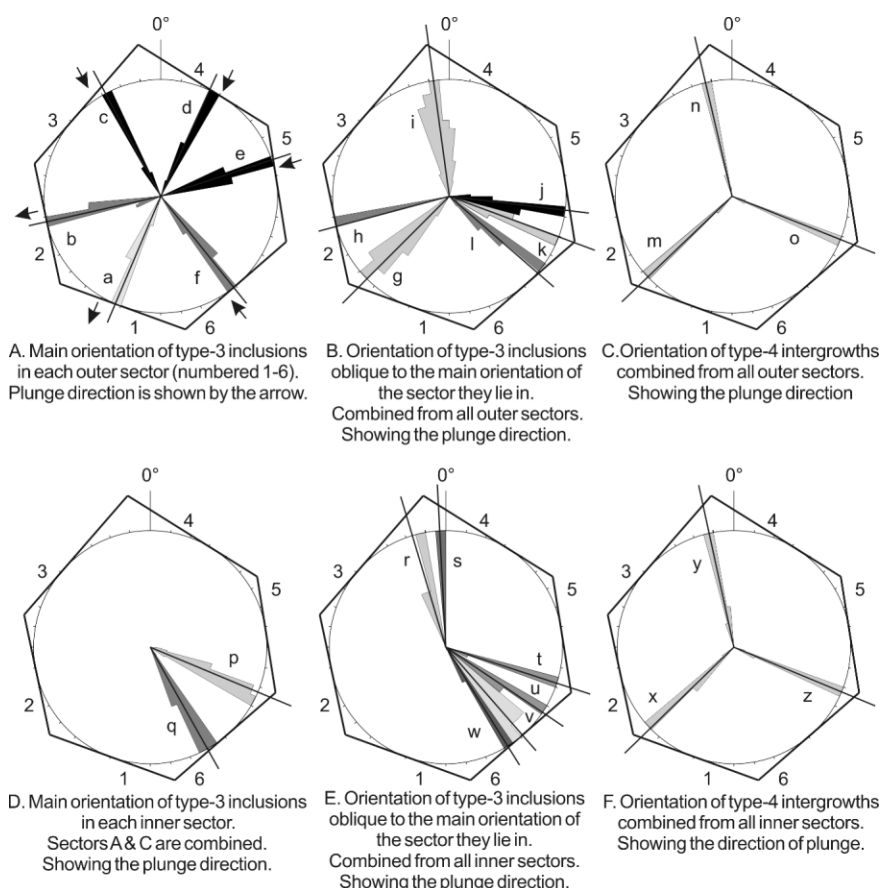F. Orientation of type-4 intergrowths combined from all inner sectors. Showing the direction of plunge.

Figure 11: Rose diagrams showing the orientation of type-3 inclusions and type-4 intergrowths in sample 03R52b.

the pre-Alpine polymetamorphic Ötztal-Stubai basement rocks from high-pressure footwall rocks of the Texel unit (Sölva et al., 2005, Habler et al., 2006). Peak Variscan metamorphic conditions of 621-708°C and 0.57-0.81 GPa, determined from garnet rim compositions, occurred at 330-345 Ma (Tropper and Recheis, 2003, Tropper and Hoinkes 1996, Hoinkes et al. 1997).

Garnets grew pre-kinematically compared to the main foliation formed of white mica, biotite and quartz. The studied porphyroblast (Fig. 10B) is 0.9 mm in diameter, sub-idioblastic and appears to comprise a single major growth zone with a very thin (<0.5 mm) sparsely developed poikiloblastic rim. The major growth zone is microstructurally zoned in two ways; sectorally and mineralogically. The former comprises a clearly texturally sector-zoned core, with a central sector(s) and six rim sectors, defined by abundant type-3 inclusions, and an outer part not obviously texturally sector-zoned. Type-4 inclusions are present through out the major growth zone, although decreasing in abundance towards the rim.

Mineralogically, the central part of the major growth zone contains relatively large (0.6 mm) elongate to equidimensional chloritoid and staurolite inclusions that define a crude planar fabric. Type-3 inclusions are absent adjacent to these inclusions, which die out towards the outer part of sector-zones 2-7 (Fig. 10B). Over the whole major growth zone, idioblastic rutile needles up to ca. 0.1 mm long and ca. 0.08 mm thick are very common (R1; Fig. 10B), dying away somewhat towards the porphyroblast rim. Locally, these seem to define a planar, and occasionally folded fabric, but mostly they have no preferred orientation. They have no effect on the orientation or abundance of the type-3 inclusions. Nearer the porphyroblast rim, large (<0.3 mm) irregular inclusions of green Fe-Ti oxides appear and still closer to the edge these are replaced by slightly larger irregular brown Fe-Ti oxides inclusions (R2, R3, respectively; Fig. 10B); neither of them defines a fabric.

In sectors 2-7, type-3 inclusion trails 0.0025 mm apart, with inclusions 0.0013 mm across, define up to four major orientations in each sector, sub-normal to the adjacent crystal face, only one of which is shown in each sector in Fig. 12E (Table 2). These cross-over, but not through, each other in the thin-section (Fig. 7F) and have a curvilinear form, rather than a straight geometry. A very large range of other orientations is present in smaller numbers within each sector, many parallel to the dominant orientations in other sectors (Fig. 12F) and often linked to longer inclusion trails (Fig. 7G). The dominant orientation gradually changes in each sector, such that the difference in orientation across sector boundaries is reduced. In the central sector, two main orientations are present (Fig. 12D, a, b). A third comprises very short type-3 inclusions, often only three or four inclusions long, indicating a very high angle to the plane of the thin-section. The wide range of orientations recorded (Fig. 12D, c-g) may be reflecting difficulties in measuring these accurately.

Backscattered electron imagery revealed an abrupt change in chemistry within sectors 2-7 (ICB, Fig. 10B), defining five perfectly planar faces. Four are coincident with the outer rim of the defined textural sector-zones whilst the fifth cuts through sectors 3 and 4, suggesting that these are one sector, with a change in dominant type-3 inclusion orientation across the sector, as in other sectors. Nearly all chloritoid and staurolite inclusions lie within this boundary. A much fainter boundary is coincident with the outer margins of textural sector zones 2-7, although type-3 inclusions are lacking in the outer area of sectors 3 and 4, and a sixth face cuts the corner of the boundary between sectors 2 and 7 (OCB, Fig 10B). A microprobe traverse indicates that the porphyroblast has a smooth Mn-bell growth zonation with antithetic Fe and Ca zoning. The innermost part of the garnet has 0.72 X_{alm}/0.16 X_{grs}. These values begin to change at the boundary of the inner and outer textural sector-zones (Ca-fall points in Fig. 10B), reaching stable values of

Rose	Sector	T4	Mean°	N	Cone°	Max %	Rose	Sector	T3	Mean°	N	Cone°	Max %
a	1	T4	353	6	7	100	*a*	1	T3	345	229	3	31
b	1	T4	059-239	16	4	59	*b*	1	T3	209	215	2	41
c	1	T4	130	18	4	56	*c*	1	T3	230	30	5	27
d	1	T4	185	2	11	50	*d*	1	T3	239	18	4	44
e	1	T4	202	1	16	100	*e*	1	T3	255	38	4	32
f	1	T4	280	3	9	67	*f*	1	T3	276	62	3	29
g	2-7	T4	353	222	1	98	*g*	1	T3	296	27	4	37
h	2-7	T4	059-239	267	1	78	*h*	2	T3	321	178	1	42
i	2-7	T4	130	260	1	75	*i*	2	T3	338	136	2	37
j	2-7	T4	184	3	9	67	*j*	3	T3	358	23	5	39
k	2-7	T4	202	46	2	96	*k*	3	T3	016	46	4	26
l	2o-7o	T4	352	63	2	92	*l*	3	T3	043	49	5	25
m	2o-7o	T4	059-239	83	2	69	*m*	4	T3	027	102	4	22
n	2o-7o	T4	130	84	2	74	*n*	4	T3	051	64	2	36
o	2o-7o	T4	186	9	5	44	*o*	5	T3	066	39	3	44
p	2o-7o	T4	202	37	3	89	*p*	5	T3	081	83	3	39
q	2o-7o	T4	279	3	9	67	*q*	5	T3	107	82	4	22
							r	5	T3	125	38	3	58
	Total N = 3,114						*s*	6	T3	145	142	2	25
							t	6	T3	170	142	3	26
							u	7	T3	218	131	1	12
							v	7	T3	233	117	2	47

TABLE 2: Distribution of type-4 intergrowths and type-3 inclusions in sample GC 1905

0.79 X_{alm}/0.07 X_{grs} at the ICB, and then changing further to 0.85 X_{alm}/0.01 X_{grs} at the OCB. Resorbtion and a second growth occurred in a thin rim zone. Thus some of the textural sector-zoning features are reflected in the chemistry.

Five faces (indicating five sectors), comparable to the ICB (Fig. 10B), appears in sections perpendicular to crystal edges in both the rhombdodecahedral and icositetrahedral forms (Figs. 1L, 3I). If the section is not exactly parallel to the edge, both forms change during growth to cut six sectors, with the new face opposite the only symmetrical sector; the OCB conforms to this. The inner sectors, which are not seen in five-sided profiles (Figs. 1L, 3I) may represents a change in crystal habit, causing a change in orientation of type-3 inclusions. Ca-Al-rich garnets tend to be rhombdodecahedral in form whilst MgAl- and Fe^{2+}Al-rich garnets tend to have an icositetrahedral habit (Rössler, 1983). Thus the gradual increase in Fe at the expense of Ca from the Ca-fall points to the ICB (Fig. 10B), coincident with the change in orientation of type-3 inclusion orientation (Fig. 12D, E), is consistent with a change from a {110} to a {211} crystal habit.

Type-4 intergrowths are 0.0013 mm wide and have the same set of orientations across the whole thin-section (Fig. 12A-C, respectively). The dominant orientations (a, b and c in Fig. 12A and the equivalents in Fig. 12B, C) lie at ca. 70° to each other. The orientation of a plunges steeply towards 353° whilst b plunges gently towards 130° and c is horizontal. As in sample ORS2b (see above),

these orientations can be matched to the A_4 rotational axes.

4. Discussion

4.1 Sector-zoning patterns and crystal orientation

The approximate orientation of a thin-section within a garnet can be established if the sector pattern is well defined by inclusions and/or intergrowths, using the axes of rotation defined by the points where the faces meet (see above). Knowing the section position within a porphyroblast is critical for modelling P-T-t paths using pseudosections (cf. Stüwe et al., 2005). For any given orientation, theoretical sector-zoning patterns predictably show increasing maximum numbers of sectors as the number of crystal faces increases. However, although most of the natural examples shown are clearly texturally sector-zoned (Fig. 5A is uncertain), the number of sectors present is usually very difficult to determine. The maximum number possible for a rhombdo-decahedral garnet is nine, as observed in Fig. 10a. For an icositetrahedral garnet the maximum possible is 17, but the most seen is 11 outer sectors and an uncertain number of inner sectors (Fig. 9C). Difficulties arise because the central zone frequently contains several small sectors (Fig. 3F, S), all with steeply dipping type-2 inclusions and/or type-3 intergrowths whilst the rim may also have several small sectors with growth directions not markedly different from adjacent sectors (Fig. 3N, R). More difficulties arise when the section is asymmetric, as is the norm, so that data from one area cannot be extrapolated to another area of the porphyroblast. Further, variations in the crystal form during growth would also result in irregular sector patterns. Thus, although in some instances the sector pattern does indicate the crystallographic orientation, relating the observed pattern to the theoretical patterns is generally not possible.

4.2 Similar microstructures from pure-shear growth

Boyle et al. (1996) noted that the stress pattern formed around a crystal growing during pure shear (Masuda and Mizuno, 1995) is comparable to that documented by Ferguson et al. (1980) during the formation of cleavage domes. Using a sample in which abundant texturally sector-zoned garnets have cleavage domes, but are wrapped by the matrix, Boyle et al. (1996) suggested that cleavage domes may form during
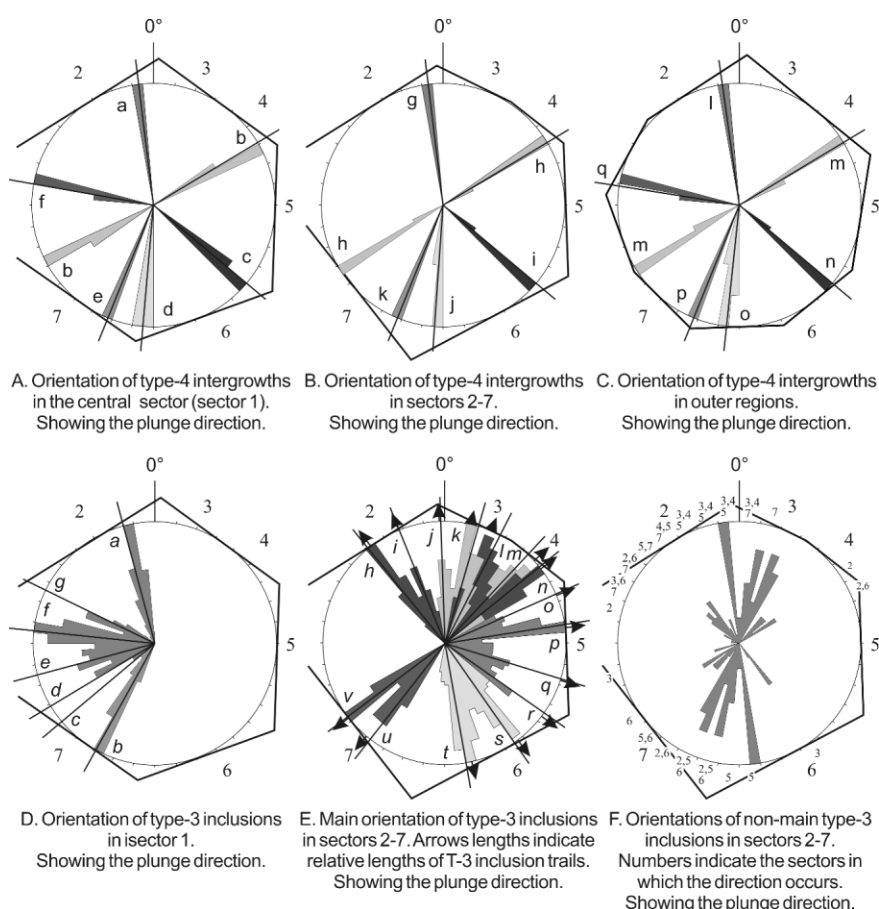

A. Orientation of type-4 intergrowths in the central sector (sector 1). Showing the plunge direction.

B. Orientation of type-4 intergrowths in sectors 2-7. Showing the plunge direction.

C. Orientation of type-4 intergrowths in outer regions. Showing the plunge direction.

D. Orientation of type-3 inclusions in isector 1. Showing the plunge direction.

E. Main orientation of type-3 inclusions in sectors 2-7. Arrows lengths indicate relative lengths of T-3 inclusion trails. Showing the plunge direction.

F. Orientations of non-main type-3 inclusions in sectors 2-7. Numbers indicate the sectors in which the direction occurs. Showing the plunge direction.

Figure 12: Rose diagrams showing the orientation of type-3 inclusions and type-4 intergrowths in sample Gc1905.

pure-shear growth. However, during pure-shear, material flows symmetrically around porphyroblast faces (sub-)normal to σ_1, with strain shadows forming adjacent to faces (sub-)parallel to σ_1. Displaced matrix material should thus be sheared away from the margin and no noticeable cleavage dome or accumulation of displaced material should develop. This is consistent with the strain pattern modelled by Masuda and Mizuno (1995). However, although they recorded a low strain zone adjacent to a spherical rigid particle in a pure shear environment, this is very narrow in relation to the size of the particle and elsewhere material was significantly displaced. In contrast, during a non-differential stress (lithostatic stress), there is no flow and hence material displaced by crystal growth accumulates at the porphyroblast margins. Thus although the stress patterns modelled by Ferguson et al. (1980) and Masuda and Mizuno (1995) are broadly similar, the causes are different and the resultant strains very different. In principle, the preservation of displaced material should indicate a lack of matrix flow and hence a non-differential stress. Although Boyle et al. (1996) argued that the porphyroblasts of their study have been wrapped by a foliation, which indicates some flow around the garnets, this seems to have had only a weak effect on the matrix, since it was insufficient to remove existing clea-vage domes. Such a weak deformation is unlikely to have formed the observed domal cleavage in their samples by the model of Matsuda and Mizuno (1995).

Note, however, that this does not imply that a porphyroblast growing during pure (or simple) shear cannot displace material, but that no direct evidence of this would be observed at the porphyroblast margin. It can be assumed that any inclusion-free porphyroblast which grew in a rock with abundant insoluble grains not involved in the porphyroblast-forming reaction has displaced the latter.

4.3 Real displacement or not?

Vernon (2004) argued that, since the layering was not de-flected by porphyroblast growth with adjacent cleavage domes (best seen in unfoliated rocks from contact metamorphic aureoles), matrix displacement does not occur. However, as noted above, a growing crystal only has to exert enough stress to cause dissolution in directly adjacent or nearby grains for insoluble material to be displaced. Displaced, insoluble grains at the porphyroblast face are essentially 'floating' in a fluid phase between the growing crystal and grains being removed by reaction and dissolution (cf. Yardley, 1974) and as it is the growth of the crystal that moves the fluid, the growth is also responsible, even if indirectly, for the displacement of the insoluble grains from their original location within the rock. Insoluble material which lies further away from the porphyroblast face will also be displaced as the stress exerted by the growing crystal is transferred through the rock, causing dissolution away from the site of crystal growth along pressure solution seams. As the matrix between the seams is removed by solution or reaction, they become closer and eventually are flattened against the porphyroblast faces, resulting in a solid accumulation of insoluble material. Essentially, displacement in 'displacement growth' refers to the motion of insoluble grains within a dissolving/reacting matrix and at the crystal margin and not to an en-bloc movement of the surrounding matrix layering.

4.4 Type-3 inclusions

In some instances, Type-3 inclusions are essentially linear and clearly define a textural sector-zoning fabric whilst in other cases they are curvilinear, with several orientations within a sector. The former have been found in conjunction with type-2 intergrowths (Fig. 9B, C, E) and the latter with type-4 intergrowths (Fig. 10A, B). Orientations within a sector may vary by 90°, although where there is more than one orientation (the maximum recorded is 14 in sector 5, Fig. 10B, Fig. 12E, F), the commoner orientations are broadly orthogonal to the sector pyramid base and vary from one sector to the next. Less common
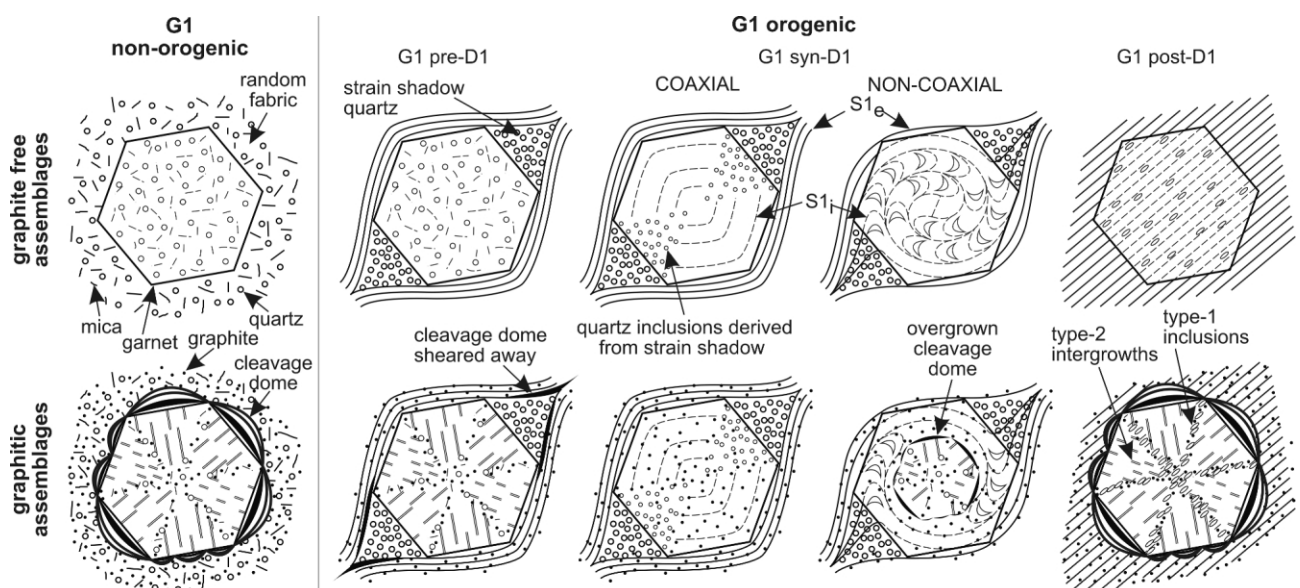

FIGURE 13: Modified Zwart diagram showing the possible occurrences of textural sector-zoning.

directions may be parallel to type-4 intergrowth directions (Fig. 11Bg, i, k and 12F) or may be parallel to common directions in other sectors, and thus be subnormal to crystal faces other than the one forming the base of the pyramid within which they grew. These atypical directions may branch directly from more common type-3 directions and may be short, consistent with them being subnormal to other crystal faces (Fig. 7H).

The spacing between trails of type-3 inclusions is less than the thickness of the thin-section, since they are frequently observed passing over/under each other. Burton (1986) suggested that texturally sector-zoned garnets grew as a series of screw dislocations (comparable to the lineages of Buerger, 1934; Petreus, 1978) with slight mis-orientations of the crystal lattice between each dislocation. Quartz could be exploiting these mis-orientations to form type-2 intergrowths and a similar mechanism for the linear trails of type-3 inclusions is possible (Fig. 9B, C, E) Extrapolating this to the more variably oriented type-3 inclusions (Fig. 10A, B) would imply that growth in these sectors was complex, but neither linear nor random.

4.5 Type-4 intergrowths

Type-4 intergrowths are similar to type-2 intergrowths in their overall elongate geometry. However, whilst the latter are often of low abundance, sometimes curved (Fig. 9D), of variable thickness (Fig. 9E) and essentially normal to the base of the pyramid within which they grew (Fig. 6), the former are, in the examples studied, very common, are invariably absolutely straight, uniformly thick and have orientations related to the crystallographic axes (especially the A_4 rotation axes), rather than any particular growth pyramid. The latter indicates that they are not reflecting textural sector-zoning as such. Whether their occurrence in texturally sector-zoned porphyroblasts is fortuitous or not is unclear. In some instances, type-3 inclusions are parallel to type-4 intergrowth directions (Fig. 11B, C). No chemical data are available from the samples studied here. Type-4 intergrowths in magmatic pegmatite garnets from the Koralpe-Saualpe basement have apatite, xenotime, rutile and kyanite compositions (Habler et al. 2007).

4.6 Deformation-metamorphism interpretations

Fig. 13 shows a modified version of part of the microstructure-porphyroblast relationship diagram proposed by Zwart (1962), showing the possible situations in which textural sector-zoning may occur in association with one or no deformation event; the latter, for example, represents contact metamorphism of undeformed metasediments. For comparison, distinction has also been made between microstructures in graphitic assemblages and non-graphitic assemblages since neither matrix displacement nor textural sector-zoning has been observed in rocks entirely lacking either graphite or carbonate as a source of carbon in the fluid phase.

Evidence of textural sector-zoning appears in only three cases. The contact metamorphic and post-D1 situations can be differentiated on the basis of the fabric seen within the type-1 inclusions. However, if intrusion into foliated rocks occurs, these become identical situations. Pre- and post-D1 growth can be distinguished by the presence or absence of cleavage domes. Where a lithostatic stress with a high fluid-pressure develops after an initial phase of garnet growth, textural sector-zoning will develop around a core containing a non sectoral inclusion pattern; both Figs. 5C and 9E show a poikiloblastic core containing evidence of one or more earlier deformation events.

A textural sector-zoning core has been shown within the non-coaxial deformation only to illustrate that this is a common observation (Fig. 5; MacQueen and Powell 1976; Bell and Hayward, 1991; Rice, 2001). In areas where spiral growth has occurred, some porphyroblasts have a texturally sector-zoned core whilst others do not; this may varying on the scale of a thin-section. Assuming that deformation started at the same time within a region, this implies a significant variation in the nucleation time of the garnets. Burton (1986) noted that the presence of carbon bearing species in a rock reduces the garnet nucleation temperature, indicating that this may also vary on small scale; a similar effect could also occur in conjunction with variations in the Mn content.

5. Conclusions

Although not rare in the Eastern- and Central Alps, textural sector-zoning and displacement growth are usually unremarked, largely because their significance is not recognised. However, the finite-element modelling of Ferguson et al. (1980) indicates that displacement growth, and thus textural sector-zoning, requires a lithostatic (non-differential) stress with a high fluid-pressure. Preservation of displaced material at a porphyroblast rim also indicates a non-differential stress during and after growth, as material flow would remove it from areas adjacent to the porphyroblast. Thus, textural sector-zoning/displacement growth is an important diagnostic feature of pre-, inter- and post-kinematic growth.

Textural sector-zoning patterns may be very complex; for mixed rhombdodecahedral-icositetrahedral garnets, up to at least 20 sectors may be present in a single section through a porphyroblast. More complex crystal habits will have more sectors. These can, in theory, be recognised from the distribution of the type-1 inclusions along sector boundaries and from variations in the orientation (in 3-D) of type-2 intergrowths and type-3 inclusion trails. In practice, sections cut close to garnet cores may have a number of small sectors which cannot be properly distinguished.

All metamorphic garnets, especially those within graphite-bearing rocks, should be carefully studied for evidence of textural sector-zoning and/or displacement microstructures. Where type-1 inclusions do not define sector boundaries clearly, high magnification and illumination are often required to see small type-2 intergrowths and type-3 inclusions; even then, they are not always easy to see. Any accumulations of graphitic material either at the margins of porphyroblasts or at the boundary of two growth zones, especially where one is inclusion-free and the other not, should be carefully studied. Finally,

the development of re-entrants at the crystal edges is a potential sign of textural sector-zoning. Since each sector grows independently, and the dominant orientation of type-2 intergrowths and type-3 inclusions is normal to the crystal face, it is clear that re-entrants are likely to form during textural sector-zoning growth.

Acknowledgements

References

Andersen, T. B. 1984. Inclusion patterns in zoned garnets from Magerøy, north Norway. Mineralogical Magazine 48, 21-6.

Bell, T. H. & Hayward, N. 1991. Episodic metamorphic reactions during orogenesis: the control of deformation partitioning on reaction sites and reaction duration. Journal of Metamorphic Geology 9, 619-640.

Bell, T. H., Johnson, S. E., Davis, B., Forde, A., Hayward, N. & Wilkins, C. 1993. Porphyroblast inclusion trail orientation data: *eppure non son girate*. Journal of Metamorphic Geology 10, 295-307.

Bolli, H., Burri, M., Isler, A., Nabholz, W., Pantic, N. K. & Probst, P. 1980. Der nordpenninische Saum zwischen Westgraubünden und Brig. Eclogae Geologicae Helvetiae 73/72, 779-797.

Bosze, S. & Rakovan, J. 2002. Surface structure-controlled sectoral zoning of the rare earth elements in fluorite from Long Lake, New York, and Bingham, New Mexico, USA. Geochimica et Cosmochimica Acta 66, 997-1009.

Boyle, A. P., Cassidy, N. & Prior, D. J. 1996. Sector-growth zoning, mica-dome development and matrix wrapping textures: implications for garnet-growth mechanisms. Abstracts from What Drives Metamorphism and Metamorphic Reactions: Heat Production, Heat Transfer, Deformation and Kinematics? Kingston University, 2 7-6.

Buerger, M. J. 1934. The lineage structure of crystals. Zeitschrift für Kristallographie 89, 195-220.

Burton, K. W. 1986. Garnet quartz intergrowths in graphitic pelites: the role of the fluid phase. Mineralogical Magazine 50, 611 20.

Carrupt, E. 2002. Geological and mineralogical study of the High Val Formozza – Binntal area (Central Alps): new stratigraphic, geochemical and structural constraints. Ph.D. Thesis, University of Lausanne, Switzerland. 185 pp.

Carrupt, E. 2003. Les textures en fleur des granats de la région du Binntal – Val Formazza (Valois, Piémont). Bulletin Murithienne 121, 43-54.

Cressey, G., Wall, F. & Cressey, B. A. 1999. Differential REE uptake by sector growth of monazite. Mineralogical Magazine 63, 813-828.

Faryad, S.W. & Hoinkes, G. 2003. P-T gradient of Eo-Alpine metamorphism within the Austroalpine basement units east of the Tauern Window (Austria). Mineralogy and Petrology 77, 129-159.

Ferguson, C. C. and Harvey, P. K. 1972. Porphyroblasts and 'crystallization force'; some new textural criteria: Discussion. Geological Society of America Bulletin 83, 3839 3840.

Ferguson, C. C., Harvey, P. K. and Lloyd, G. E. 1980. On the mechanical interaction between a growing porphyroblast and its surrounding matrix. Contributions to Mineralogy and Petrology 75, 339 52.

Frank, W., Höck, V. & Miller. Ch. 1987. Metamorphic and tectonic history of the Central Tauern Window. In Flugel, H. W & Faupl, W. (eds.) Geodynamics of the Eastern Alps. Deutike, 34-54.

Gauchat, K. & Baumgartner, L. 2006. Sector zoning in garnets as growth mechanism indicator. 4th Swiss Geoscience Meeting, Bern. 2pp.

Gaides, F., Abart, R., de Capitani, C., Schuster, R., Connolly, J. A. D. & Reusser, E. 2006. Characterization of polymetamorphism in the Austroalpine basement east of the Tauern Window using garnet isopleth thermobarometry. Journal of Metamorphic Geology 24, 451-475.

Gregurek, D., Abart, R. & Hoinkes, G. 1997. Contrasting Eoalpine P-T evolution in the southern Koralpe, Eastern Alps. Mineralogy and Petrology 60, 61-80.

Habler, G. 2004. Exhumation in the eo-Alpine high-pressure belt of the Eastern Alps: Petrological, structural and geochronological investigations of high-pressure metamorphic rocks. PhD thesis Department of Geological Sciences, University of Vienna, Vienna.

Habler, G. & Thöni, M. 1998. New petrological and structural data from the eclogite bearing polymetamorphic eastern Austroalpine basement nappes (NW Saualpe, Austria). Freiberger Forschungshefte C 471, 86-88.

Habler G & Thöni, M. 2001. Preservation of Permo-Triassic low-pressure assemblages in the Cretaceous high-pressure metamorphic Saualpe crystalline basement (Eastern Alps, Austria). Journal of Metamorphic Geology 19, 679-697.

Habler, G., Thöni, M. & Sölva, H. 2006. Tracing the high pressure stage in the polymetamorphic Texel Complex (Austroalpine basement unit, Eastern Alps): P-T-t-d constraints. Mineralogy & Petrology 88, 269-296.

Habler, G., Thöni, M. & Miller, C. 2007. Major and trace element chemistry and Sm-Nd age correlation of magmatic pegmatite garnet overprinted by eclogite-facies metamorphism. Chemical Geology, in press.

Harker, A. 1932. Metamorphism. A study of the transformation of rock-masses. Methuen, London. 362 pp.

Hoinkes, G., Thöni, M., Lichem, C., Bernhard, F., Kaindl, R., Schweigl, J., Tropper, P. & Cosca, M. 1997. Metagranitoids and associated metasediments as indicators for pre-Alpine magmatic and metamorphic evolution of the western Austroalpine Ötztal Basement (Kaunertal, Tirol). Schweizerische Mineralogische und Petrographische Mitteilungen 77, 299-314.

Holland, T. J. B. & Powell, R. 1998. An internally consistent thermodynamic data set for phases of petrological interest. Journal of Metamorphic Geology 16, 309-343.

Hollister, L. S. & Gancarz, A. J. 1971. Compositional sector-zoning in clinopyroxene from the Narce area, Italy. Amercian Mineralogist 56, 959-979.

Konzett, J. & Hoinkes, G. 1996. Paragonite-hornblende assemblages and their petrological significance: an example from the Austroalpine Schneeberg Complex, Southern Tyrol; Italy. Journal of Metamorphic Geology 14, 85-101.

Kouchi, A., Sugawara, Y., Kashima, K. & Sunagawa, I. 1983. Laboratory growth of sector zoned clinopyroxenes in the system $CaMgSi_2O_6 - CaTiAl_2O_6$. Contributions to Mineralogy & Petrology 83, 177-184.

Kwak, T. A. P. 1981. Sector-zoned $annite_{85}phlogopite_{15}$ micas from the Mt. Lindsay Sn-W-F(-Be) deposit, Tasmania, Australia. Canadian Mineralogist 19, 643-650.

Leute, M. A. 2000. Mineralogische Charakterisierung der Radentheiner und Zillertaler Schmuckgranate, Österreich. Diplomarbeit, Universität Wien. 129 pp.

MacQueen, J. A. & Powell, D. 1976. Relationships between deformation and garnet growth in Moine (Precambrian) rocks of western Scotland. Geological Society of America Bulletin 88, 235-240.

Masuda, T. & Mizuno, N. 1995. Deflection of pure-shear viscous flow around a rigid spherical body. Journal of Structural Geology 17, 1615-1620.

Miller, C., Thöni, M., Konzett, J., Kunz, W., Schuster, R. 2005. Eclogites from the Koralpe and Saualpe type-localities, Eastern Alps, Austria. Mitteilungen der Österreichischen Mineralogischen Gesellschaft 150: 227-263.

Misch, P. 1971. Porphyroblasts and 'crystallization force': some textural criteria. Geological Society of America Bulletin 82, 245-251.

Passchier, C. W., Trouw, R. A. J., Zwart, H. J. & Vissers, R. L. M. 1993. Porphyroblast rotation: *eppur si muove?*. Journal of Metamorphic Geology 10, 283-294.

Passchier, C. W. & Trouw, R. A. J. 1996. Microtectonics. Springer, Heidelberg. 289 pp.

Pestal, G., Brüggemann-Ledolter, M., Draxler, I., Eibinger, D., Eichberger, H., Reiter, C. & Scevik, F. 1999. Ein Vorkommen von Oberkarbon in den mittleren Hohen Tauern. Jahrbuch der Geologischen Bundesanstalt Österreich 141, 491-502.

Petreus, I. 1978. The divided structure of crystals I. Lineage and sectoral structure in pyrite and beryl. American Mineralogist 63, 725-731.

Phillips, W. J. & Phillips, N. 1980. An Introduction to Mineralogy for Geologists. John Wiley, Chichester. 352 pp.

Raisin, C. A. 1901. On certain altered rocks from near Bastogne and their relation to others in the district. Quarterly Journal of the Geological Society of London 57, 55-72.

Reeder, R. J. & Protsky, J. L. 1985. Compositional sector-zoning in dolomite. Journal of Sedimentary Petrology 56, 237-247.

Rice, A. H. N. 1993. Textural and twin sector-zoning and displacement of graphite in chiastolite and pyralspite and grandite garnets in the Varscides of south-west England. Proceedings of the Ussher Society 9, 124-131.

Rice, A. H. N. 2001. Displacement textures (cleavage domes) and sector-zoning as hydrostatic stress indicators in contact and regional metamorphic terranes. At EUG 11, Strasbourg. Journal of Conference Abstracts 6, 666.

Rice, A. H. N. 2007. Chemical disequilibrium during garnet growth: Monte Carlo simulations of natural crystal morphologies: Comment. Geology in press.

Rice, A. H. N. & Mitchell, J. I. 1991. Porphyroblast textural sector-zoning and matrix displacement. Mineralogical Magazine 55, 379-396.

Rössler, H. J. 1983. Lehrbuch der Mineralogie. VEB Deutscher Verlag für Grundstoffindustrie, Leipzig. 833 p.

Schuster, R. & Frank, W. 2000. Metamorphic evolution of the Austroalpine units east of the Tauern Window: indications for Jurassic strike-slip tectonics. Mitteilungen der Gesellschaft der Geologie- und Bergbaustudenten Österreich 42 (1999), 37-58.

Schuster, R., Hoinkes, G., Kaindl, R., Koller, F., Leber, T., Puhl, J. & Bernhard, F. 1999. Metamorphism at the eastern end of the Alps - Alpine, Permo-Triassic, Variscan? Berichte der Deutschen Mineralogischen Gesellschaft, Beiheft zum European Journal of Mineralogy 11, 111-136.

Schuster, R., Scharbert, S., Abart, R. & Frank, W. 2001. Permo-Triassic extension and related HT/LP metamorphism in the Austroalpine - Southalpine realm. Mitteilungen der Gesellschaft der Geologie- und Bergbaustudenten in Österreich 44, 111-141.

Schuster, R., Koller, F., Hoeck, V., Hoinkes, G. & Bousquet, R. 2004. Explanatory notes to the map: Metamorphic Structure of the Alps. Metamorphic Evolution of the Eastern Alps. Mitteilungen der Österreichischen Mineralogischen Gesellschaft 149, 175-199.

Selverstone, J. & Munoz, J. L. 1987. Fluid heterogeneities and hornblende stability in interlayered graphitic and non-graphitic schists (Tauern Window, Eastern Alps). Contributions to Mineralogy & Petrology 96, 426-440.

Shelley, D. 1972. Porphyroblasts and 'crystallization force': some new textural criteria: Discussion. Geological Society of America Bulletin 83, 919-920-1202.

Sölva, H., Grasemann, B., Thöni, R. C., & Habler, G. 2005. The Schneeberger Normal Fault Zone: Normal faulting associated with Cretaceous SE-directed extrusion in the Eastern Alps (Italy/Austria). Tectonophysics 401, 143-166.

Spear, F. S. 1993. Metamorphic Phase Equilibria and Pressure-Temperature-Time Paths. Mineralogical Society of America Monograph. 799 pp.

Spry, A. 1972. Porphyroblasts and 'crystallization force': some new textural criteria: Discussion. Geological Society of America Bulletin 83, 1201-1202.

Stüwe, K., Robl, J. and Hauzenberger, C. 2005. Interpreting zoning profiles in minerals: The sectioning effect. Geophysical Research Abstracts 7, 03358.

Thöni, M. 1999. A review of geochronological data from the Eastern Alps. Schweizerische Mineralogische und Petrographische Mitteilungen 79, 209-230.

Thöni, M. 2002. Sm-Nd isotope systematics in garnet from different lithologies (Eastern Alps): age results, and an evaluation of potential problems for Sm-Nd chronometry. Chemical Geology 185, 255-281.

Thöni, M. & Miller, C. 1996. Garnet Sm-Nd data from the Saualpe and the Koralpe (Eastern Alps, Austria): chronological and P-T constraints on the thermal and tectonic history. Journal of Metamorphic Geology 14, 453-466.

Thöni, M. & Miller, C. 2000. Permo-Triassic pegmatites in the eo-Alpine eclogite-facies Koralpe complex, Austria: age and magma source constraints from mineral chemical, Rb-Sr and Sm-Nd isotope data. Schweizerische Mineralogische und Petrographische Mitteilungen 80, 169-186.

Tropper, P. & Hoinkes, G. 1996. Geothermobarometry of Al_2SiO_5 bearing metapelites in the western Austroalpine Ötztal basement. Mineralogy and Petrology 58, 145-170.

Tropper P. & Recheis, A. 2003. Garnet zoning as a window into the metamorphic evolution of a crystalline complex: the northern and central Austroalpine Ötztal-Complex as a polymetamorphic example. Mitteilungen der Oesterreichischen Geologischen Gesellschaft 94, 27-53.

Vance, D. & O'Nions, R. K. 1992. Prograde and retrograde thermal histories from the Central Swiss Alps. Earth and Planetary Science Letters 114, 113-129.

Vernon, R. H. 2004. A Practical Guide to Rock Microstructures. Cambridge University Press, Cambridge. 594 pp.

Yardley, B. W. D. 1974. Porphyroblasts and 'crystallization force': discussion of some theoretical considerations. Geological Society of America Bulletin 85, 61 62.

Zwart, H. J. 1962. On the determination of polymetamorphic mineral associations and its application to the Bosot area (central Pyrenees). Geologische Rundschau 52, 38-65.

Zwicky, F. 1929. On the imperfections of crystals. Proceedings of the National Academy of Sciences, United States 15, 253-259.

A. Hugh N. RICE[1),*)], Gerlinde HABLER[2)], Elisabeth CARRUPT[3)], Gianluca COTZA[1)], Gerhard WIESMAYR[4)], Ralf SCHUSTER[5)], Helmut SÖLVA[6)], Martin THÖNI[2)] & Friedrich KOLLER[2)]

[1)] Department of Geodynamics and Sedimentology, Geozentrum, Althanstraße 14, 1090 Vienna, Austria.

[2)] Department of Lithospheric Research, Geozentrum, Althanstraße 14, 1090 Vienna, Austria.

[3)] Department of Geology, University of Lausanne, Lausanne, Switzerland.

[4)] Rohöl-Aufsuchungs AG, Schwarzenbergerplatz 16, A-1015 Vienna, Austria.

[5)] Geologisches Bundesanstalt, Neulinggasse 38, 1031 Vienna, Austria.

[6)] Institute of Earth Sciences, University of Graz, Heinrichstraße 26, 8010 Graz, Austria.

[*)] Corresponding author, alexander.hugh.rice@univie.ac.at